Office of Research and Sponsored Programs

Hydrate Flow Performance JIP

Risk-based restarts of untreated subsea oil and gas flowlines in the GoM

Final Project Report

By

Dr. Michael Volk, Emmanuel Delle-Case

&

Douglas Estanga

March 2007

MMS #1006CT39690

Table of contents

List of figures

List of tables

1. Executive summary

Production shut-ins are part of any oil production operation, whether they are scheduled shut-ins to allow for maintenance or unplanned shut-ins in case of failure or emergency. In the Gulf of Mexico, shut-ins are necessary when hurricanes approach. After a hurricane, production systems are restarted following strict procedures to prevent the formation of hydrates and to prevent the formation of hydrate plugs. Some of these procedures involve flushing the lines with dead oil or inhibitors prior to shut-in or restart. In some cases, it is believed that the fluid properties combined with a proper selection of restart parameters may allow restart operations to be conducted safely without implementing these special procedure steps. Practically, this means that oil could be brought back into production faster, resulting in additional revenue for the operating companies. In the case of major hurricanes such as Rita or Katrina, a faster ramp-up of oil production also means that the supply of oil to the market would be less affected.

A lot of work is currently devoted to the understanding and modeling of hydrate formation in pipeline under steady-state conditions. Very little work has been done or published on hydrate formation and plug development during restart operations. This work intends to fill up this knowledge gap a little more. The purpose of this study is to conduct experiments to verify if and under what conditions restarts could be performed safely without the deployment of inhibitors or special operational steps to prevent plugging. Experiments were conducted to investigate the effect of restart rate, water cut, liquid loading and oil-water distribution on the plugging tendency of crude oil–water systems upon restarts. Multiphase pumping restarts in horizontal pipes and gas-dominated restarts in low spots were conducted. Comparisons were made with simulation tools as well.

Main findings show that the presence of a segregated water phase, as opposed to dispersed water phase, increases the severity of plugging, as well as an increase in water cut. Higher velocities seem to decrease the plugging severity; the decrease was more efficient in dispersed cases. Salinity had a positive effect in the sense that hydrate formation rate was reduced and/or plug permeability was higher with higher salt concentration. A mechanism of hydrate plug formation was observed, where hydrates are observed to creep up the pipeline. Finally, anti-agglomerant were proven to be an effective way to prevent plugging, even after a 5-day shut-in with a hydrate slurry already present in the line. However, to be effective, the inhibitor has to be injected prior to shut-in to be properly dispersed in the water phase upon restart.
Comparisons with transient flow simulations (without hydrate module) show that the initial water distribution is fairly well predicted, except for higher water cuts (more than 50%). However, after forming hydrates, simulations fail to predict the location of the water because of the complexity of the resulting flow patterns. A hydrate formation module such as CSMHYK-OLGA should be used to compare the experimental results with the predictions.

Finally, a risk analysis methodology is being developed from the findings of this study; being in its preliminary stages, it is not reported here but will be made available upon completion. Overall, this study highlighted the complexity of the transient hydrate formation process and demonstrated that a thorough knowledge of the complex oil-water-gas transient flow patterns is required to achieve successful understanding and modeling of hydrate plug development in pipelines under transient conditions. A new facility is being designed at the University of Tulsa to more realistically conduct experiments in geometries representing real production systems (jumpers, manifolds, risers), as well as expanding the range of parameters being tested, such as the gas restart rate or fluid warm-up during restart conditions.

2. Introduction

In the last ten hurricane seasons, $178.4 billion have been reported as losses. Last year alone, the oil industry incurred $8 billion in structural damages. This $8 billion does not account for productivity losses or any other subsequent problem originating from the hurricanes. In fact, a Congressional Budget Office report estimated that a comprehensive repair to the energy infrastructure in the Gulf of Mexico would cost $18 to $31 billion. With 6 to 8 hurricanes predicted for the East coast for the 2006 season, there is a concern that many operators will be forced to shut down and evacuate their facilities many times again this season. After these shutdowns, production lines must be restarted and the fear of hydrate formation and plugging becomes the number one flow assurance issue.

Most deepwater operators have developed strict shutdown and restart procedures to avoid hydrate formation upon restart. The flow lines are typically inhibited by circulation of hot stabilized crude, methanol injection or by the use of anti-agglomerants. These restart procedures take time to implement – 24 hours or more for circulation of hot crude – and require the hydrate prevention systems to be functional, which may not always be the case after a hurricane. In other cases, extreme conditions generated by hurricanes exceed the design parameters of the facilities and, as a result, prevention systems fail or even undergo structural damages (e.g. ingress of sea water after pipeline rupture). Smaller independent operators may not even be aware of the hydrate plugging potential on restart or may not have the adequate teams to evaluate the risks to make educated decisions. Improper evaluation of these risks may result in flow line plugging that will require many days or weeks to clear, further delaying oil production.

Nowadays, one of the primordial goals in the flow assurance field is to optimize the time required to bring oil production to pre-hurricane levels – and therefore minimize the disruption of the country's supply – by better understanding the risk of hydrate plugging. With confidence that the flow lines could be restarted safely without deploying the typical hydrate prevention methods, large operators could restore peak oil production in minimal time. Smaller operators could utilize the guidelines for their restart resulting in a reduced proportion of plugged pipe lines. Procedures to restart a flowline without inhibition can only be obtained through a combination of research and field experience. Results from this JIP have shown that hydrate formation is minimal during shutdown but will occur very rapidly upon restart. Results also indicate that the hydrate formation rate increases as the fluid velocity increases, but that the plugging tendency is reduced. Recent results – also confirmed by other studies in DeepStar – stress the importance of the oil-water distribution (i.e. segregated vs. dispersed) on the plugging tendency of a system, but this relationship is not very well understood. These findings suggest that there may be an optimum restart procedure to minimize the hydrate plugging risk and that this procedure would involve the restart rate as well as knowing the distribution of the fluids inside the flow line (some fluids may segregate over long shut-in times).

This project was divided in two phases. Phase I focuses on validating the concepts explained above, i.e. the effect of phase distribution and demonstrate the existence of an optimum restart rate. Phase II focuses in greater detail on some of the parameters which could potentially affect the findings from Phase I, such as liquid loading, salinity and water cut. The expected outcome of this research is a set of conclusions and guidelines helping the operators to better manage the hydrate risk upon restart of uninhibited flow lines. Since the focus of this study is the feasibility of restarting flow lines without deploying the hydrate prevention equipment, combined with selection of the appropriate restart rate, these guidelines for restart could be deployed in the field almost immediately without additional investments from operators.

3. Objectives

As mentioned in the introduction, the project was divided in two phases. The purpose of Phase I of this study was to validate key concepts related to restart of uninhibited flow lines. Specifically, the focus was to:

- demonstrate the existence of an optimum restart rate capable of preventing plugging in a non-inhibited flowline,
- demonstrate how the presence of a free water phase can influence the plugging tendency of a system, and
- generate restart data in low spots where production fluids accumulate and evaluate the plugging tendency of such systems under gas-dominated restarts, which is often the case when wells are restarted after a production shut-in.

Phase II was aimed at studying the effect of other parameters, especially on low spot restarts. The parameters of interests were liquid loading in low spot, water cut, salinity and anti-agglomerant.

4. Facility set-up

4.1 Description

The hydrate facility was donated by Marathon to the University of Tulsa in June 2001. Relocation of the flow loop, process building and control trailer occurred in the summer of 2002 and commissioning occurred in the summer of 2003.

The facility consists of a 3” pipe flow loop mounted on an 80-ft long tilt table. The flow path is 160-ft long and fluids can be set in motion by a Leistritz twin-screw multiphase pump or by the rocking motion of the flow loop deck. The process building contains all the equipment necessary to charge oil, water, gas and additives into the flow loop. The control trailer contains all the data acquisition modules and the operator computer interface. A 40’x 30’ contained storage slab is used to store the test fluids. A boiler system has been added to the original facility as well as a boiler room. An overview of the facility is shown on Figure 4.1.

Figure 4.1: Overall view of hydrate facilities

4.2 Flow loop

The flow loop consists of a 3” schedule 80 stainless steel long pipe connected at both ends to the suction and discharge sides of a multiphase pump. The pipe forms a closed flow path in which fluids are introduced and is jacketed with a 5” schedule 10 stainless steel pipe over most of its length except around the multiphase pump. Figure 4.2 shows a schematic of the flow loop. The entire flow loop is mounted on an 80-ft long deck that can be rocked back and forth with a maximum amplitude of +/- 8 degrees and a minimum period of 30 seconds to set the fluid in motion in a rocking mode. The fluids can be also pumped with the Leistritz twin-screw multiphase pump from horizontal up to 8 degrees uphill (the pump does not operate with a downhill discharge to prevent it from running dry). The maximum flow rate displaced by the pump is about 250 gpm, which corresponds to about 12 ft/s maximum fluid velocity. The pump suction and discharge pressures are measured as well as the pressure drops across each leg and the overall pressure drop. Several temperature probes are mounted on the outside pipe wall of the inner pipe and measure the outside wall temperature of the process pipe. Glycol is used as a coolant in the annulus and can be set to flow co-current or counter-current with respect to the process fluids. Inlet and outlet temperatures of the coolant are measured and the average glycol temperature is used to control cooling ramps to impose to the facility. A 20-ton chiller is used to cool the glycol. The glycol flow rate is also measured and is maintained constant during each test. Four view ports at the beginning and end of each leg are used to observe the hydrate formation. These view ports are made up of three sapphire windows at 120 degrees angle of each other around the pipe. Video systems allow us to record videos of the hydrate formation and dissociation. Three gamma densitometers are also used to collect density data of the process fluids. Additionally, a scanning-densitometer allows measurement of the density profile on 40-ft of the discharge leg of the flow loop, allowing precise plug identification.

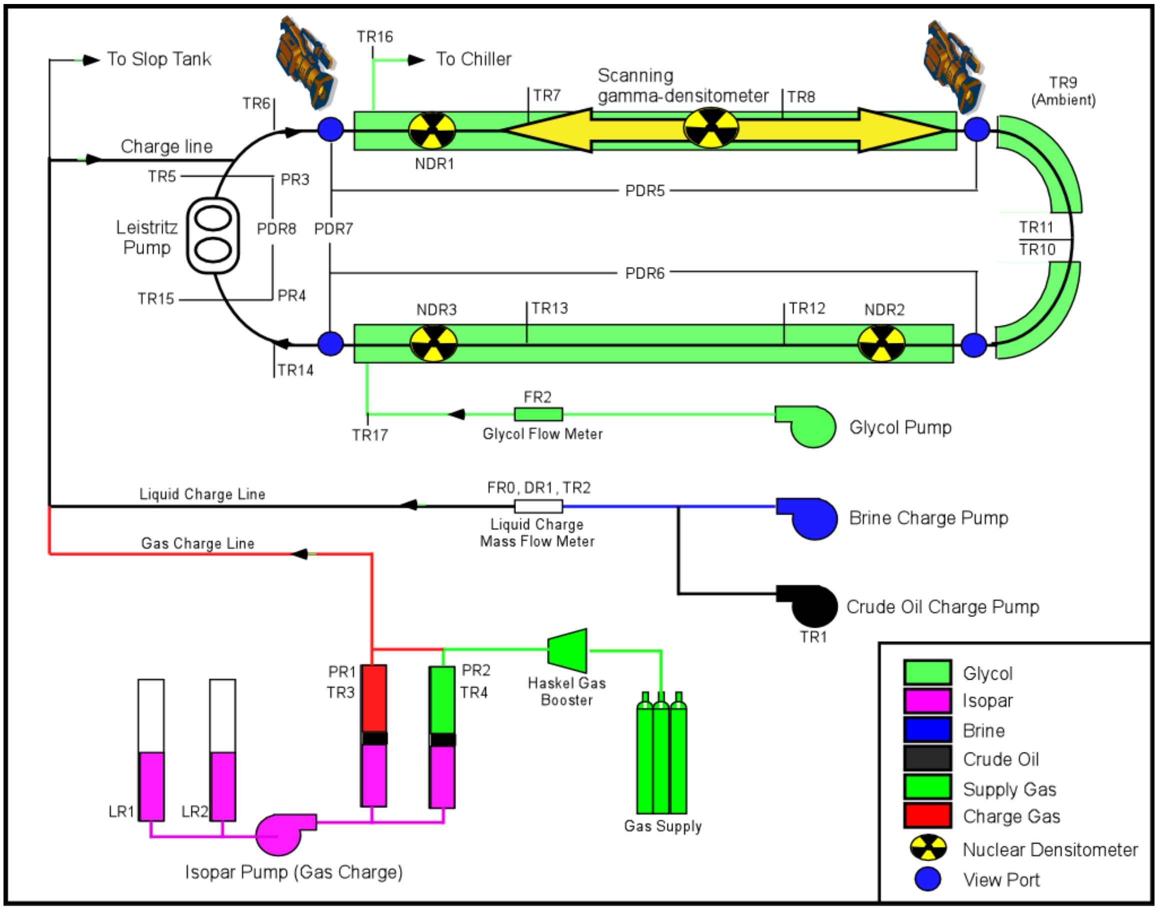

Figure 4.2: Schematic of the hydrate facility

4.3 Low spot test rig

Due to terrain configuration, many pipelines have low spots where significant amounts of water may accumulate. Low spots in jumper lines and manifolds may also be critical to restart because of the amount of water that can be found. Restart of wells usually starts with large amounts of gas produced; when the gas hits the low spots, several scenarios may occur. If the gas rate is fast enough, hydrates will form rapidly but water in the low spots may be evacuated and re-dispersed downstream of the low spot; however, if the gas rate is too slow, the water will remain in the low spot, hydrate formation will be slower but the large retention time of the water will favor plug formation. To conduct low spot experiments, the flow loop will be inclined in order to create a low spot where natural gas will be circulated at various restart rates using a CNG compressor and/or CNG trailer. Figure 4.3 shows a schematic of the modified facility. In this configuration, the multiphase pump is taken out of the facility and the ends of the flow loop are flanged off.

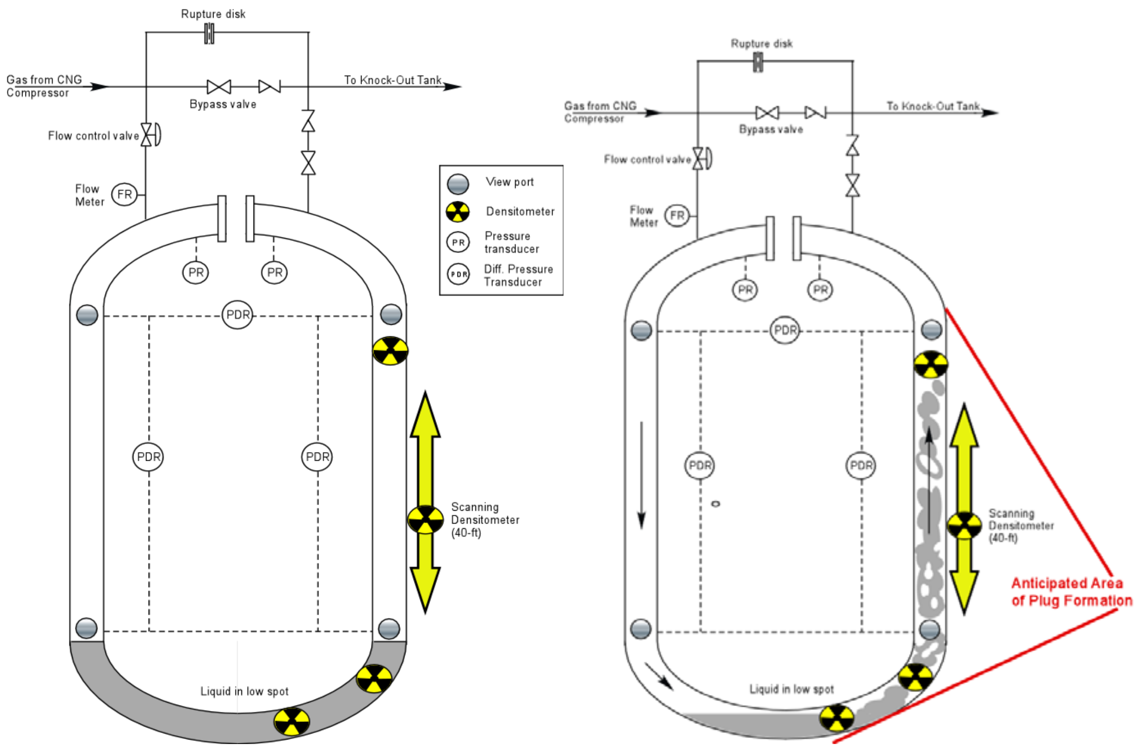

(a) (b)

Figure 4.3: (a) Facility modified for low spot b) Hydrate plug generation

In a typical low spot test, water and oil will be charged into the flow loop at the low spot and the fluids will be cooled statically into the hydrate region. A CNG compressor will allow circulation of natural gas through the fluids accumulated in the low spot. Hydrate formation rates and plug formation will be monitored through pressure measurements, a scanning gamma-densitometer and view ports on the uphill leg of the flow loop. Should a plug form, evaluation of the plug permeability will be possible knowing the gas flow rate through the plug and the differential pressure across the plug. Plug length will be evaluated using the scanning gamma-densitometer.

4.4 Auxiliary equipment

Liquid charge systems

Brine, oil, solvents and additives can be charged from the equipment in the process building. Typically, oil, brine and solvents are charged into the flow loop at low pressure using gear pumps. The amount of each phase loaded in the flow loop is measured by a Micro Motion mass flow meter and recorded by the computer system. Water and additives can also be injected while the facility is pressurized at a very slow rate using a Milton-Roy high pressure piston pump. A brine preparation system is used to prepare brines from tap water prior to injection into the flow loop. Crude oil is circulated and heated prior to injection into the flow loop to insure dissolution of any precipitated material such as paraffins. The charge lines are heat-traced and insulated to prevent freezing, gelling and/or wax deposition.

Gas charge system

Gas is introduced into the flow loop by volumetric displacement using high-pressure cylinders and a high-pressure piston pump. Two cylinders are used alternatively, one being charged from the gas supply while the second is being transferred into the flow loop. The gas is being withdrawn from a natural gas supply trailer and boosted up to 2,000 psia into the high pressure cylinders. To charge the flow loop the gas from one cylinder is being displaced by pumping Isopar oil on the other side of the piston using the high-pressure piston pump. Pressure and temperature of the gas leaving the cylinder is measured as well as the displaced volume of Isopar oil; the mass of gas introduced into the flow loop is then computed using equations of state and input compositions. The system allows use of the Peng-Robinson (PR), Redlich-Kwong (RK) or Benedict-Webb-Rubbin (BWR) equations of state in the gas mass computation. The gas addition system can be set to operate to charge a given mass of gas into the system and/or maintain a set pressure into the flow loop. For constant pressure tests, the measured amount of gas injected into the facility is a measurement of the hydrate formation.

Seal oil system

A John Crane seal oil system is used to maintain back-pressure on the multiphase pump seals as well as provide cooling and lubrication. This seal system constantly adjusts the back-pressure on the seals to track the flow loop pressure. An accumulator also keeps the pressure on the seals in case of a power failure, allowing sufficient time for the operators to depressurize the flow loop and bring the system to a safe condition.

Cooling system

A 20-ton chiller is used to cool down the glycol that circulates in the annulus. The glycol is also used to cool down the seal oil and the video equipment. Temperature ramps can be programmed up to about 40ºF/hr. The glycol is circulated using a centrifugal pump and the glycol flow rate is measured with a magnetic flow meter. A second holding tank equipped with steam coils and another centrifugal pump is used to hold and circulate glycol at temperatures higher than 85ºF. A shell-tube steam heat exchanger is also used to heat up the glycol circulating in the annulus during the hydrate dissociation phase.

Boiler system

Steam is required as a heat source in this facility for the purpose of controlling flow loop temperature, especially during hydrate dissociation phase as well as provide heat tracing for the liquid charge lines and avoid plugging or freezing during winter conditions. A 450,000 Btu/hr boiler was purchased and installed in a boiler room. The boiler room also hosts a 25 HP air compressor to actuate the control valves, sump pump and gas booster.

Instrumentation

The flow loop is instrumented mainly with Rosemount pressure and differential pressure transducers and Omega temperature transducers (RTDs). A Micro Motion Coriolis flow meter records the amounts of liquids charged into the flow loop. The location of these instruments is also shown on Figure 4.2.

Table 4.1 provides a list of the principal instruments on the facility. The location of these instruments is also shown on Figure 4.2.

NAME	DESCRIPTION	Range
AI1	Loop Inclination Angle	-166.6 - +166.6 deg
DR1	Micro Motion Density	0 - 1.2 g/cc
FR2	Glycol Flow Meter (Fisher)	0 - 583.3 gpm
LR1	Isopar Tank A Level (DP)	0 - 33.3 "H2O
LR2	Isopar Tank B Level (DP)	0 - 33.3 "H2O
NDR1	Nuclear Density Gauge #1	0 - 1.2 g/cc
NDR2	Nuclear Density Gauge #2	0 - 1.2 g/cc
NDR3	Nuclear Density Gauge #3	0 - 1.2 g/cc
PDR4	John Crane Seal Differential Pressure	0 - 200 psi
PDR5	Loop Differential Pressure East	0 - 36 psi
PDR6	Loop Differential Pressure West	0 - 36 psi
PDR7	Loop Differential Pressure	0 - 36 psi
PDR8	Leistritz Differential Pressure	0 - 36 psi
PR1	Piston Vessel A Gas Pressure	0 - 3,000 psia
PR2	Piston Vessel B Gas Pressure	0 - 3,000 psia
PR3	Loop Inlet Pressure (Leistritz Discharge)	0 - 2,500 psia
PR4	Loop Outlet Pressure (Leistritz Suction)	0 - 2,500 psia
PR5	John Crane Pump Seal Pressure	0 - 2,500 psia
TR02	Micro Motion Temperature	-50 - +250 F
TR03	Piston Vessel A Temperature	0 - 200 F
TR04	Piston Vessel B Temperature	0 - 200 F
TR05	Loop Temperature @ 1.3-ft from Pump Discharge	0 - 200 F
TR06	Loop Temperature @ 6.3-ft from Pump Discharge	0 - 200 F
TR07	Loop Temperature @ 27.1-ft from Pump Discharge	0 - 200 F
TR08	Loop Temperature @ 51.9-ft from Pump Discharge	0 - 200 F
TR09	Ambient Temperature	0 - 200 F
TR10	Loop Temperature @ 80.5-ft from Pump Discharge	0 - 200 F
TR11	Loop Temperature @ 88.3-ft from Pump Discharge	0 - 200 F
TR12	Loop Temperature @ 109.1-ft from Pump Discharge	0 - 200 F
TR13	Loop Temperature @ 133.7-ft from Pump Discharge	0 - 200 F
TR14	Loop Temperature @ 154.9-ft from Pump Discharge	0 - 200 F
TR15	Loop Temperature @ 159.7-ft from Pump Discharge	0 - 200 F
TR16	East Jacket Glycol Temperature	0 - 200 F
TR17	West Jacket Glycol Temperature	0 - 200 F
TR18	Seal Oil Temperature South	0 - 200 F
TR19	Seal Oil Temperature North	0 - 200 F

Table 4.1: Main instruments on the facility

5. Test fluids and operating procedures

5.1 Test fluids

Several fluids have been used in this project. Two crude oils and a model oil. Caratinga oil is a Campos Basin fluid with an API density of about 25. This crude oil presents the characteristic of forming very stable emulsions; therefore, it was possible to conduct restart experiments with both a segregated water phase (charged without mixing) or a dispersed water phase (created by running the oil-water mixture through the pump). Another crude oil, called Buttermilk, is a GoM fluid operated by BP. This fluid was selected to provide data with anti-agglomerants since it had been studied in a previous phase of the JIP.
The model oil utilized was Citgo 19, which presents the characteristic of flowing as an oil-water dispersions but segregates readily upon shut-in. The model oil allows for valuable visual observations that are not possible in crude oil systems.

The water phase used in this study was either fresh tap water or a brine, reconstituted by mixing different amount of sodium chloride (NaCl) with fresh tap water.

The gas phase used in all these experiments is Tulsa City natural gas whose average composition is given in Table 5.1 below:

Component	Mole (%)
N2	1.05
CO2	1.23
C1	94.84
C2	2.35
C3	0.38
C4+	0.15
Total	**100**

Table 5.1: Natural gas composition

Finally, the anti-agglomerant selected was Armoclear 2550 from Akzo-Nobel, a water-dispersible quaternary ammonium compound, used in many commercial anti-agglomerants.

5.2 Operating procedure

For all tests, the following procedure was implemented. First the flow loop is vacuumed to 28” Hg, prior to being charged with a pre-determined amount of oil and water. Then the loop is pressurized to a test pressure of either 1,000 psig for low spot tests, or 2,000 psig for pumping restarts. After a stabilization period to ensure that the system is leak free and to ensure saturation of the oil phase with gas, the flow loop is set static at the desired inclination angle and the fluids are cooled down at a rate of 40°F/hr. After the pre-determined shut-in time (typically three hours) and after the system has entered the hydrate formation region, the restart is carried out using either the multiphase pump for pumping restarts or using natural gas from a CNG compressor for the gas dominated low-spots restart experiments. Pumping tests were restarted for 12 hours while low-spots tests where restarted for shorter period of times (30 minutes to one hour). This shorter period of time was initially dictated by the flaring capacity of the system, which was increased to one hour for later tests.

After the restart period, hydrates are dissociated by increasing the system temperature and the gas being released is measured. Finally the loop is depressurized and cleaned with solvents.

5.3 Charge considerations

To simulate dispersed vs. segregated conditions, Caratinga crude oil was used since it exhibits stable oil-water dispersions when mixed. In both cases though, the crude oil has to be saturated with gas before the experiment can start. If not, the initial gas uptake will be due to under-saturation of the oil rather than hydrate formation and data will be misinterpreted. Since the saturation process can only practically be achieved by mixing, to achieve both segregated and dispersed conditions with an equally gas-saturated oil phase required two different charge procedures. For dispersed case, oil and water were charged, then gas was added to pressurize the flow loop while the fluids were in motion (either by rocking of pumping). This procedure is not suitable to maintain a segregated water phase. For segregated cases, the oil only was charged and the flow loop was pressurized with gas and set in motion to saturate the oil phase. After saturation of the oil was achieved, the motion was stopped, the flow loop set in the desired position and the water phase was added using a high pressure piston pump. After water injection, the flow loop remained static to insure the water phase remained segregated.

5.4 Water conversion calculations

For closed systems, which were the case for rocking and pumping tests, the water calculation is calculated using the amount of gas consumed during the experiment. However, for low spots tests and gas dominated restarts, the system is an open system. Even though the gas flow rate going into the loop is measured, there is no measurement of the gas going out. Even if available, this measurement would not be accurate enough to measure the amount of gas consumed by the hydrate formation process. Therefore, water conversion calculations had to be carried out in a different way. This new calculation procedure was developed during the project so only a few water conversion calculations are available. In this new procedure, after restart, the flow loop was depressurized to the initial pressure before restart. Then, the flow loop was heated up and the loop pressure allowed to increase. The pressure increase is related to both thermal expansion and gas released fro m dissociating hydrates. After dissociation, this excess gas was transferred into a gas cylinder - placed on a scale - until the loop pressure was back to pressure and temperature prior to the cooling (or shut-in) phase. The cylinder weight was measured and this excess gas corresponds to the mass of gas consumed by hydrates.

6. Experimental results

A total of 49 tests were conducted. Fourteen were restart tests (rocking or pumping) in the standard flow loop configuration, while 35 were gas dominated restarts in low spots. Table 6.1 lists the total number of tests conducted in this study along with test conditions.

Caratinga oil was mainly selected to conduct segregated and dispersed experiments since it is the only crude available to exhibit both behavior depending on the charging procedure. The model oil Citgo 19 was selected to conduct most of the tests to visually observe the phenomena as well as to eliminate any chemistry effect due to the complex composition of crude oils. Finally the Buttermilk crude oil was selected to conduct tests with anti-agglomerants since chemical dosage was available from past laboratory experiments.

Test ID	Phase Distribution	Water Cut (% Vol.)	Restart conditions		
			Angle (deg.)	Velocity (ft/s)	Type
Natural gas only					
NG 08	-	100	-8	0.15	Pumping
NG 09	-	100	-8	0.25	Pumping
NG 10	-	100	-8	0.25	Low Spot
NG 11	-	100	-5	0.25	Low Spot
Caratinga crude oil					
CA 10	Segregated	25	-8	-	Rocking
CA 11	Dispersed	25	-8	-	Rocking
CA 12	Dispersed	50	-8	0.15	Low Spot
CA 13	Dispersed	50	-8	0.25	Low Spot
CA 14	Segregated	50	-8	0.15	Low Spot
CA 15	Segregated	50	-8	0.25	Low Spot
CA 16	Segregated	50	-8	0.25	Low Spot
CA 17	Segregated	25	-8	0.25	Low Spot
CA 18	Segregated	25	0	7.2	Pumping
CA 19	Dispersed	25	0	7.2	Pumping
CA 20	Segregated	25	0	0.6	Pumping
CA 21	Dispersed	25	0	0.6	Pumping
CA 22	Segregated	25	0	3.9	Pumping
CA 23	Dispersed	25	0	3.9	Pumping
CA 24	Segregated	50	0	0.6	Pumping
CA 25	Dispersed	50	0	0.6	Pumping
CA 26	Segregated	50	0	3.9	Pumping
CA 27	Dispersed	50	0	3.9	Pumping
CA 28	Dispersed	25	-8	0.15	Low Spot
CA 29	Dispersed	50	-8	0.15	Low Spot
Citgo 19 model oil					
MO 08	Segregated	50	-8	0.25	Low Spot
MO 09	Segregated	50	-8	0.15	Low Spot
MO 10	Segregated	25	-8	0.15	Low Spot
MO 11	Segregated	25	-8	0.25	Low Spot
MO 12	Segregated	12.5	-8	0.15	Low Spot
MO 13	Segregated	12.5	-8	0.25	Low Spot
MO 14	Segregated	50*	-8	0.15	Low Spot
MO 28	Segregated	50	-8	0.25	Low Spot
MO 28R	Segregated	50	-8	0.25	Low Spot
MO 29	Segregated	5	-8	0.15	Low Spot
MO 30	Segregated	5	-8	0.25	Low Spot
MO 31	Segregated	75	-8	0.15	Low Spot
MO 32	Segregated	75	-8	0.15	Low Spot
MO 33	Segregated	75	-8	0.25	Low Spot
MO 34	Segregated	50*	-8	0.15	Low Spot
MO 35	Segregated	50*	-8	0.15	Low Spot
MO 36	Segregated	50*	-8	0.15	Low Spot
Buttermilk crude oil					
BM 18	Segregated	35	-8	0.15	Low Spot
BM 3A	Segregated	35	-8	0.15	Low Spot
BM 4A	Segregated	35	-8	0.15	Low Spot
BM 3AR	Segregated	35	-8	0.15	Low Spot
BM 5A	Segregated	35	-8	0.15	Low Spot
BM 6A	Segregated	35	-8	0.15	Low Spot
BM 7A	Segregated	35	-8	0.15	Low Spot
BM 8A	Segregated	35	-8	0.15	Low Spot

* Salinity tests

Table 6.1: Overall experimental test matrix

6.1 Effect of phase distribution

Several tests were conducted to investigate the effect of phase distribution. Some tests were conducted rocking while others were conducted pumping. The most representative tests are the rocking ones since for pumping tests, the segregation effect is masked by the pumping which tends to create a dispersion.

The rocking tests are presented in Table 6.2 and discussed below. The effect of phase segregation on pumping tests is discussed in the next section while discussing the effect of restart rate.

Test ID	Phase distribution	Water cut (% Vol.)	Liquid loading (% Vol.)
CA 10	Segregated	25	50
CA 11	Dispersed	25	50

Table 6.2: Phase distribution experiments

For the rocking tests, plugging tendencies with segregated phases appeared to be worse than dispersed conditions, as illustrated in Figure 6.1 and 6.2. These figures show the fluctuations in density measurements as the loop is rocked back and forth and the fluids move from one side to the other. Figure 6.1 shows the traces for the segregated conditions and figure 6.2 the traces for dispersed conditions.

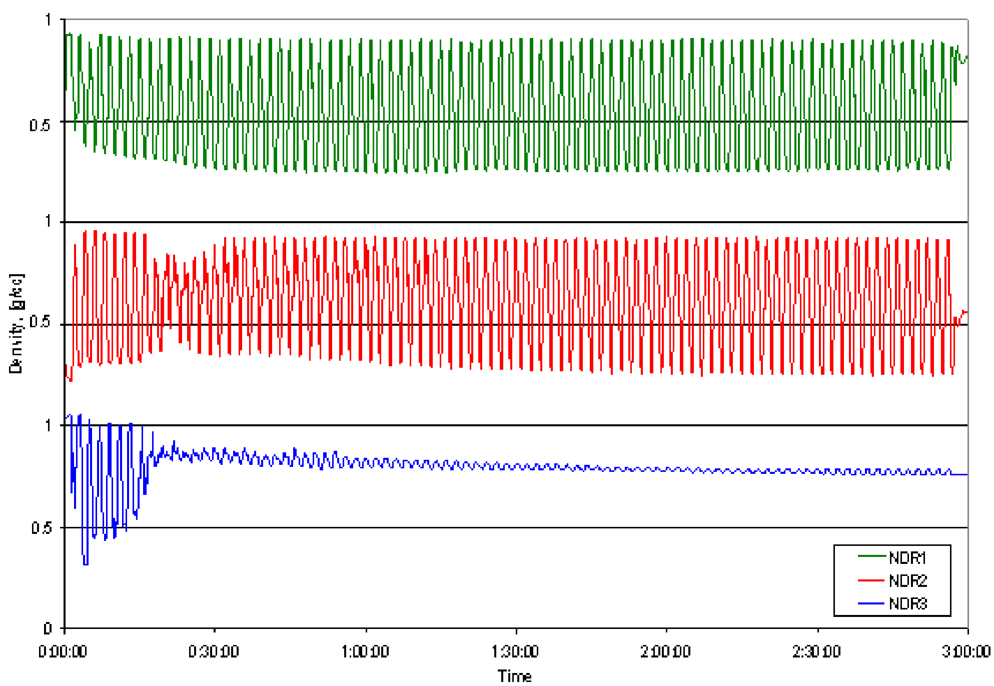

Figure 6.1: Density traces for segregated restart case

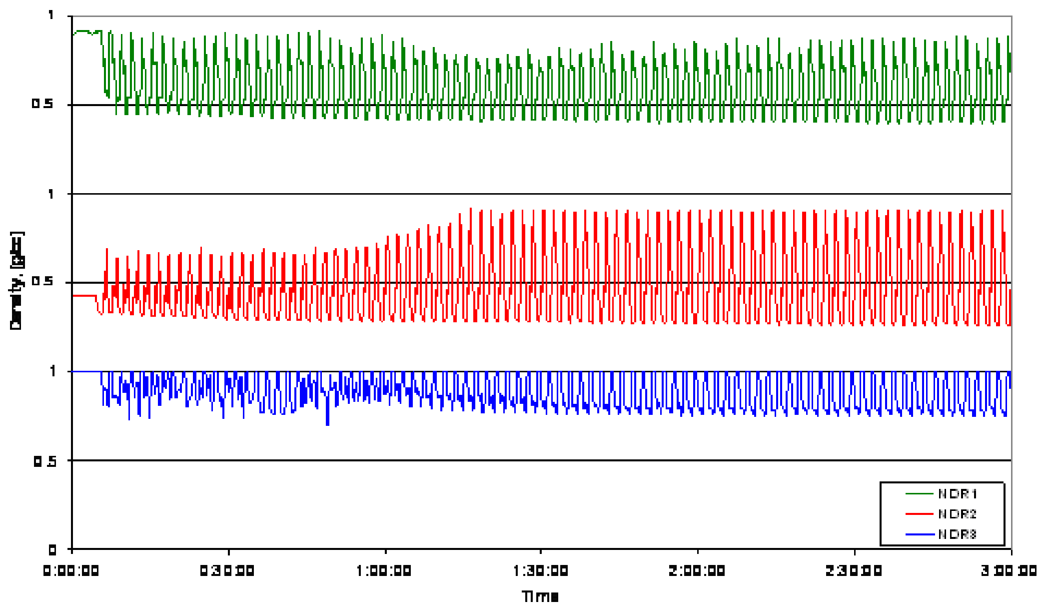

Figure 6.2: Density traces for dispersed restart case

As can be seen in Figure 6.1, the fluctuations completely cease within 30 minutes into the restart as indicated by NDR3 density trace. On the other hand, for the dispersed case, fluctuations remain visible throughout the test. Their amplitude decrease due to an increase in the viscosity of the slurry formed but overall, the fluids remain in motion. The scanning-densitometer trace indicated that a large restriction formed in the suction leg of the flow loop. This is shown in Figure 6.3 where the liquid level measured after restart is less than pre-restart level, indicating that some material accumulated as hydrates in the other leg (suction leg). This is confirmed by the NDR3 density trace (suction leg) in Figure 6.1. This was not observed for the dispersed case.

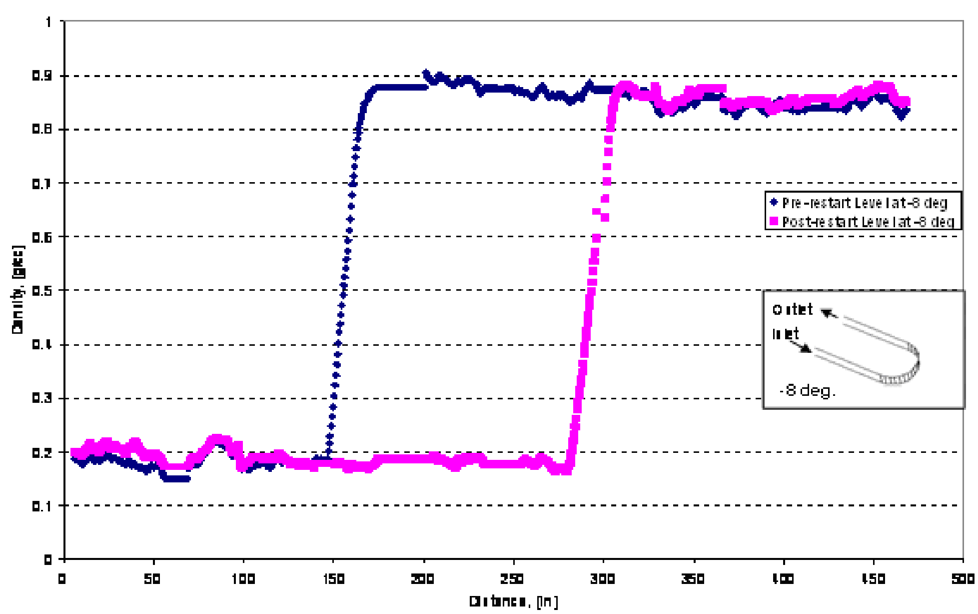

Figure 6.3: Liquid level measured by scanning-gamma densitometer for segregated case

Figures 6.4 and 6.5 show the water conversions for these two tests. During the shut-in phase, very little water converts into hydrates. Most of the hydrate formation takes place upon restart. Under segregated conditions, about 65% of the water was converted into hydrates as opposed to about 12% only for the dispersed case.

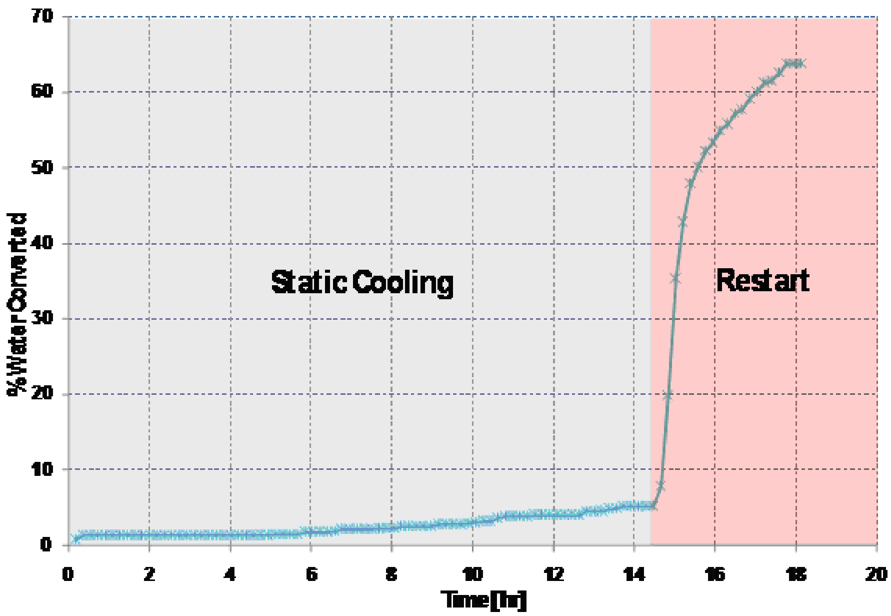

Figure 6.4: Water conversion calculations – Segregated restart case

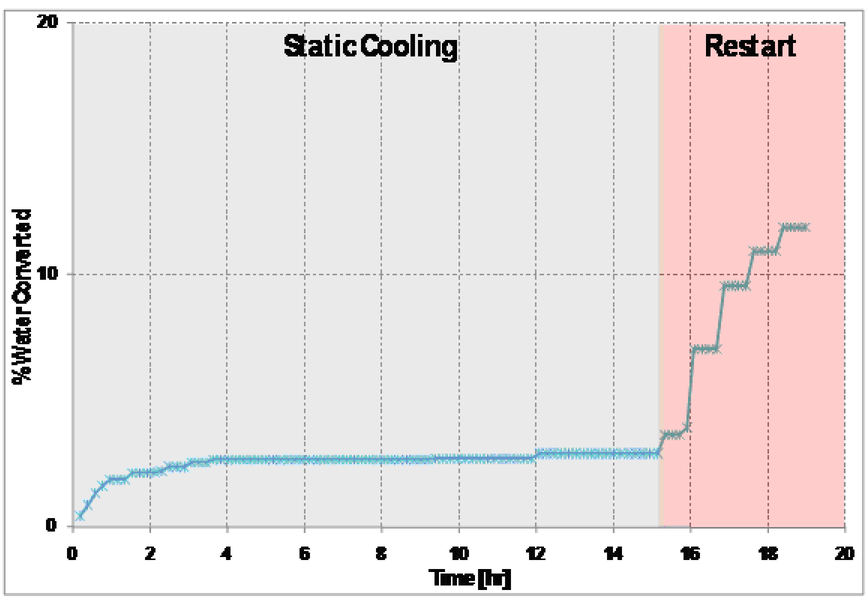

Figure 6.5: Water conversion calculation – Dispersed restart case

It is not clear why the dispersed case lead to lower water conversion than the segregated case, but mass transfer limitations may be at play. Under dispersed conditions, a hydrate shell forms around the water droplet and reduces further growth by isolating the occluded water from the gas phase. For the segregated phase, hydrate conversion occurs in the bulk of the water phase, resulting in a higher conversion rate.

These two experiments suggest that the presence of a free segregated water phase is more critical for restart. This trend was confirmed in the restart rate tests presented next, as well as the gas-dominated restart experiments in low spots.

6.2 Effect of restart rate

Companies follow strict operating procedures when restarting wells. Primary concern is the inhibition of the flow line to prevent hydrates and another parameter is the restart rate of the well. The goal is to bring the well back on stream in the minimum amount of time, but also restart rates are limited to avoid sanding of the wells. It was hypothesized prior to this work, that there may be an optimum restart rate for which the risk of hydrate plugging could be minimized without injecting hydrate inhibitors. This section describes the experiments conducted to investigate the effect of restart rate on the plugging potential of an untreated crude oil system.

In this series of experiments, the flow loop was shut-in horizontal at 2,000 psia, and cooled down to 40°F. The restart was conducted with the multiphase pump at different speeds, corresponding to different mixture velocities. Caratinga crude oil was used for this phase and the effect of segregated vs. dispersed water phase was also investigated. Table 6.2 shows the test matrix for the restart rate effect. All tests were conducted with fresh water, 50% liquid loading, 5°F/hr cooling rate and in constant pressure mode (i.e. with gas addition).

Test #	Water cut (% Vol.)	Mixture velocity (ft/s)	Phase distribution
CA-20	25	0.6	Segregated
CA-22		3.9	
CA-18		7.2	
CA-21		0.6	Dispersed
CA-23		3.9	
CA-19		7.2	
CA-24	50	0.6	Segregated
CA-26		3.9	
CA-25		0.6	Dispersed
CA-27		3.9	

Table 6.3: Experiments for effect of restart rate

At 25% water cut and under rocking conditions, the flow loop plugged so this water cut was investigated first. However, under pumping conditions, this water cut did not create any blockage, so the water cut was increased to 50%. Figures 6.6 and 6.7 show the pressure drops traces for the 25% and 50% water cut cases respectively.

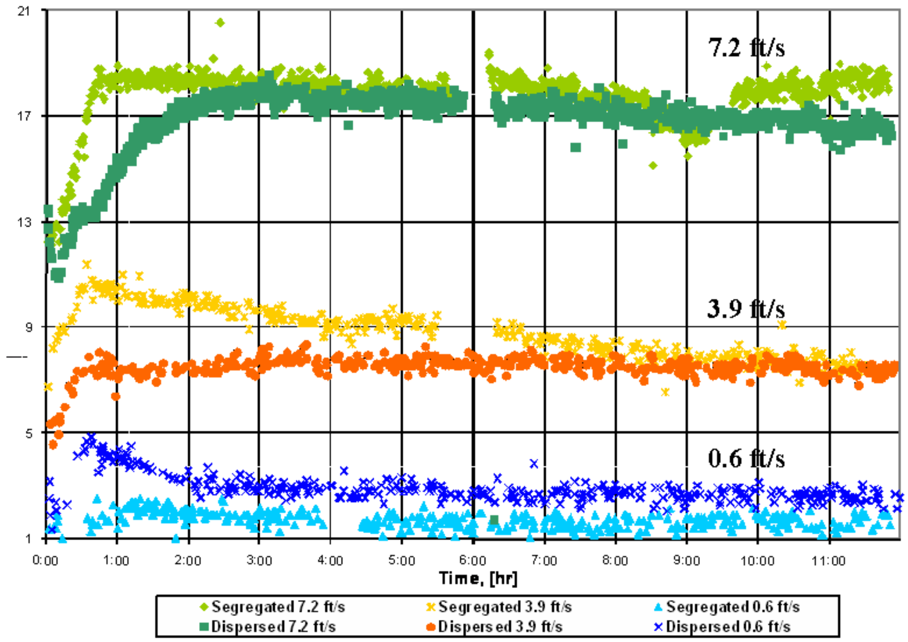

Figure 6.6: Pressure drop during restart (25% water cut)

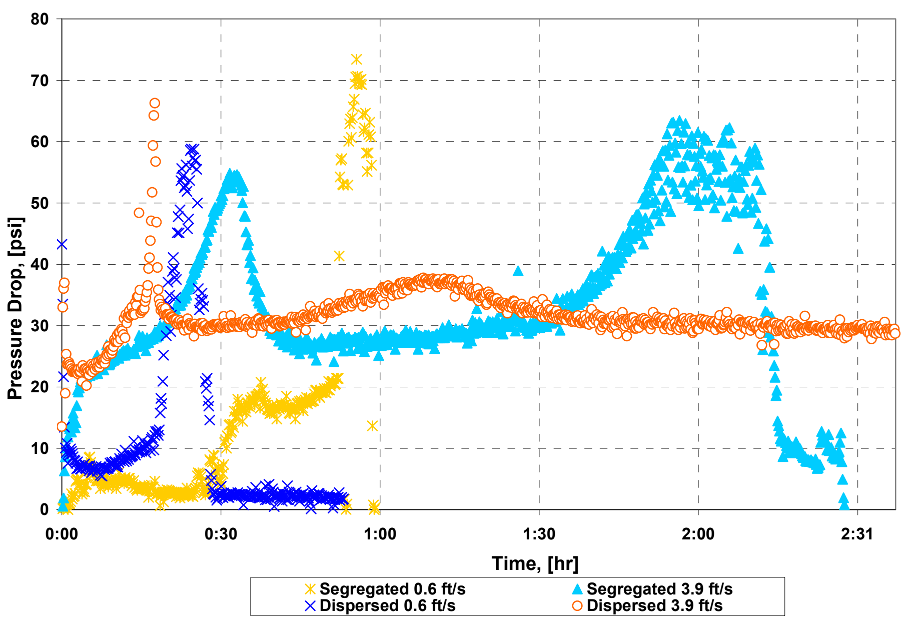

Figure 6.7: Pressure drop during restart (50% water cut)

For the 25% water cut (non-plugging cases), the pressure drop remains fairly constant throughout the test. The segregated cases show a higher initial pressure drop which eventually stabilizes around the same value as shown by the dispersed cases. This is believed to be due to the difference in flow patterns: the oil-water segregated flow pattern is more complex and exhibits a higher pressure drop, but eventually the water is re-dispersed into the oil and this difference disappears. None of these tests plugged.

As can be seen on Figure 6.7, the pressure drop for the 50% water cut cases shows a much higher pressure drop than the non-plugging cases. The plugging typically occurs in two steps: initially, the pressure drop and the solid concentration increase as hydrates are formed; a rapid increase in pressure drop is seen as significant agglomeration takes place and plugging occurs. At this time, the test must be aborted to avoid damage to the facility, especially to the pump. Among these 50% water cut cases, only three resulted in plugging: these are the low velocity cases (both dispersed and segregated) and the 3.9 ft/s segregated case. The 3.9 ft/s dispersed case was a marginal pass and the hydrate slurry was circulated for the entire restart duration (12 hours). This is an indication that dispersed phase conditions combined with a higher mixture velocity reduced the plugging tendency.

These experiments also show that for both segregated conditions, a higher mixture velocity reduced the risk of plugging. For the segregated cases, plugging occurred after 1 hour for the 0.6 ft/s case, whereas for a velocity of 3.9 ft/s the plugging time was delayed until 2 hours. For dispersed conditions, a velocity of 0.6 ft/s resulted in plugging after 30 minutes while 3.9 ft/s prevented plugging altogether. Also, it is interesting to notice that for both 3.9 ft/s cases (dispersed and segregated), a first increase in pressure drop can be seen (after 15 minutes and 30 minutes respectively); this increase only lasts temporarily and eventually the pressure drop goes back down. A possible explanation is that hydrates started agglomerating but there was enough energy from the pump to re-disperse these agglomerates, at least for some time. This is not seen for the low velocity cases.
Unfortunately, no data is available for the higher velocity cases (7.2 ft/s) at 50% water cut since pump failure occurred before these tests could be conducted.

The optimum restart rate could not be identified with the available data but these restart rate experiments indicate that higher velocities are beneficial to reduce the plugging tendency. In other words, the lower the velocity, the higher the plugging tendency of the system. They also confirm that for dispersed case the plugging tendency is also reduced. Higher velocity data (7.2 ft/s) should be conducted for 50% water cuts and other fluids should be tested to confirm these trends.

6.3 Gas dominated restarts in low spots without inhibitors

Low spots are frequently encountered in production systems. One example is in jumpers between wellhead and manifold. These jumpers are also more prone to plugging since they usually have a faster cool down time and smaller diameter than the main flow lines. A series of experiments was therefore dedicated to simulate a low-spot configuration, as described in section 4.3.

As previously mentioned, the low spot experiments were conducted under gas restart. Liquid or multiphase restarts in low spots could not be conducted because of the impossibility to run the pump in this configuration. The gas restart rate tested was 0.15 and 0.25 ft/s. The rate is limited to the CNG compressor output and the fact that the system operates in an open system configuration with gas being flared. Higher gas rates would require longer pipe lengths as well as a recirculation system for the gas phase. The gas rates tested are more representative of actual leaks through valves than actual well restart conditions.

6.3.1. Effect of restart rate and water cut

As mentioned before, the two restart rates tested were 0.15 and 0.25 ft/s gas velocity. Different water cuts ranging from 5 to 75% were also tested. Table 6.3 shows the test matrix for the restart rate experiments.

Test ID	Phase distribution	Water cut (% Vol.)	Velocity (ft/s)	Oil Phase
NG 08	-	100	0.15	-
NG 09			0.25	
CA 12	Dispersed	50	0.15	Caratinga
CA 13			0.25	
CA 14	Segregated		0.15	
CA 15			0.25	
MO 29	Segregated	5	0.15	Citgo 19
MO 30			0.25	
MO 12		12.5	0.15	
MO 13			0.25	
MO 10		25	0.15	
MO 11			0.25	
MO 09		50	0.15	
MO 08			0.25	
MO 31		75	0.15	
MO 33			0.25	

Table 6.4: Effect of restart rate test matrix for low spot tests

Table 6.3 shows that these tests also correspond to different water cut and phase distribution. Figure 6.8 below shows the maximum pressure drop recorded for these experiments, which is an indication of the plugging tendency of the system. All these experiments resulted in the formation of restrictions in the line, even though the gas flow was never affected. The restrictions formed were permeable to gas but not to liquid.

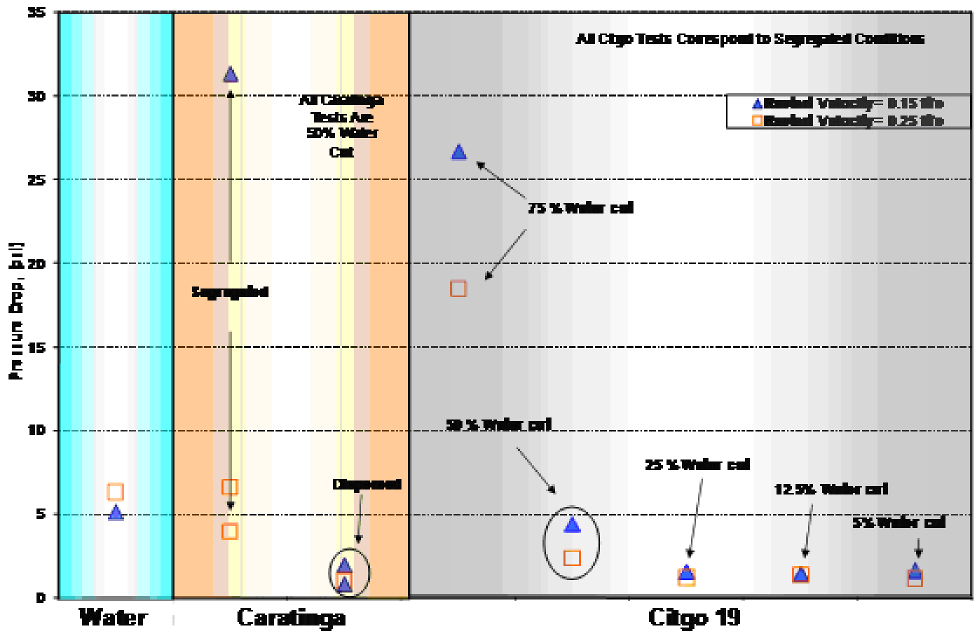

Figure 6.8: Maximum pressure drop for low spot experiments – Effect of restart rate and water cut

As shown in Figure 6.8, for the model oil Citgo 19, the pressure drop increases with water cut. As expected, higher water cuts increase the plugging potential and result in higher pressure drops. At lower water cuts, below 50%, the pressure drops remain low and not much difference is observed between the lower and higher velocity cases. The velocities used in this study are so close that no significant difference is found until a significant water cut is reached. Above 50% water cut, the higher velocity decreases the pressure drop in the system.

Also for Caratinga tests, no effect of velocity was found on the dispersed case conditions. However, for segregation conditions, an effect of velocity was observed, with higher velocity, here again reducing the plugging tendency. These observations may be explained by the complexity of flow patterns and rheology for the high water cut cases and/or segregated cases. For dispersed cases or low water cuts, the mixture is more homogeneous and the flow patterns are less complex therefore the experiment outcome could be less affected by the velocity difference. For the 100% water cut cases, no significant difference was observed between high and low velocity. Finally, with the 5% water cut, the amount of hydrate present in the system is too low to allow the detection of any agglomeration. There was no evidence that restrictions were formed or if they were, no impact could be seen on pressure drop.

Overall, these experiments confirmed that low velocities tend to increase the plugging tendency as does the presence of a segregated water phase. They also pointed out the necessity to understand the complex three phase (oil-water-gas) transient flow patterns in order to understand the mechanisms of hydrate plug formation.

6.3.2. Effect of salinity

Real production systems almost never produce fresh water, but brines of different salinities. The thermodynamic impact of salt is relatively well known and understood. However, the impact of salinity on hydrate kinetics, agglomeration and plug formation is not understood. Four tests were conducted to investigate the impact of salinity on the plug development during restart in low spots. The model oil Citgo 19 was selected to allow visual observation and also eliminate other chemistry effects – besides the presence of salt – that would result from the use of crude oils. Table 6.4 shows the test matrix for the salinity experiments.

Test ID	Salinity (% wt.)
MO-09	0.0
MO-36	3.5
MO-34	7.0
MO-35	14.0

Table 6.5: Salinity test matrix

These tests were conducted with 50% water cut to allow most of the restrictions to be covered by the visual ports and scanning gamma-densitometer. The lower restart velocity of 0.15 ft/s was selected since it is the most stable and easier to maintain, coming directly from the natural gas compressor.

These four tests were very important as they highlighted the mechanism of hydrate plug formation and explained how the liquid and solid redistribute along the pipe during restart. The mechanism taking place during these experiments is described below in Figures 6.9a to 6.9g.

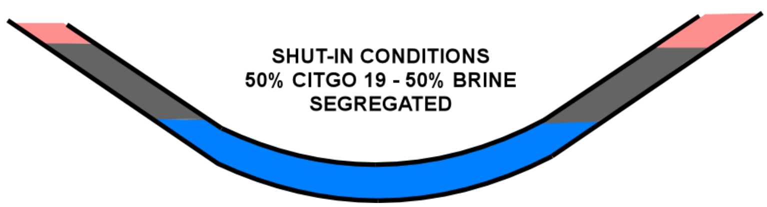

Figure 6.9a: Before hydrate formation, water, oil and gas form segregated phases in the low spot.

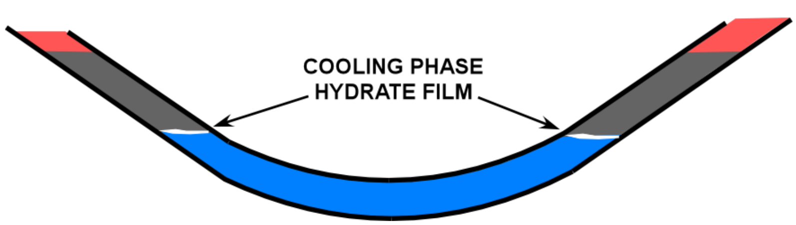

Figure 6.9b: After reaching the hydrate formation region, a thin film of hydrates might form at the oil-water interface. Hydrate formation is minimal when the system is static.

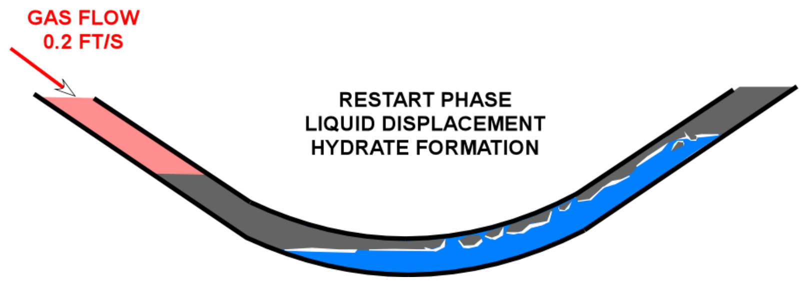

Figure 6.9c: Upon restart, the oil and water phases are displaced; hydrates form rapidly as turbulence in the system is increased.

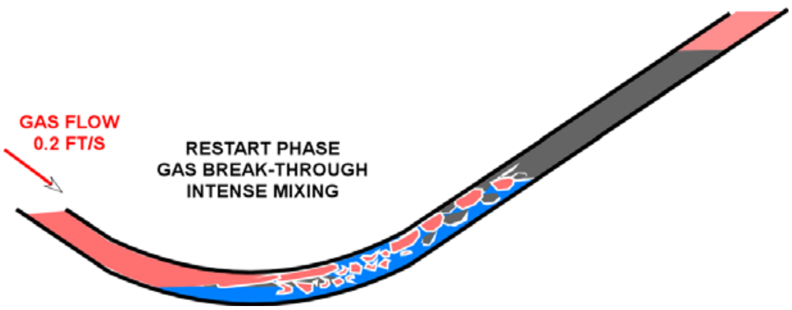

Figure 6.9d: When the gas phase reaches the low spot, gas bubbles break through the liquid column and the increased mixing and contact between phases increases hydrate formation rate. Gas bubbles breaking through the water phase get coated by a thin film of hydrates to form gas "balloons".

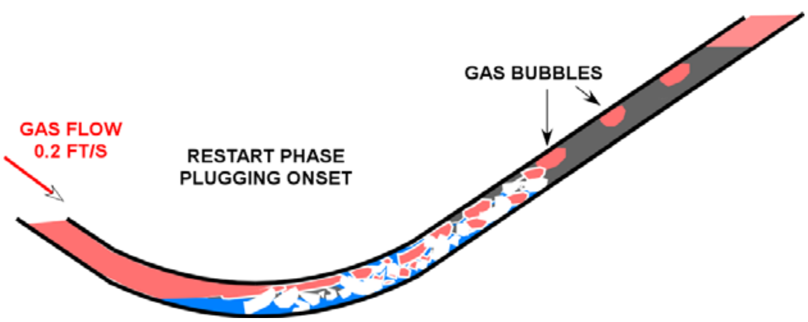

Figure 6.9e: As more of these gas "balloons" break through the water column, they break and contact more water, therefore forming hydrate agglomerates. The amount of hydrates increases very fast towards the formation of a plug.

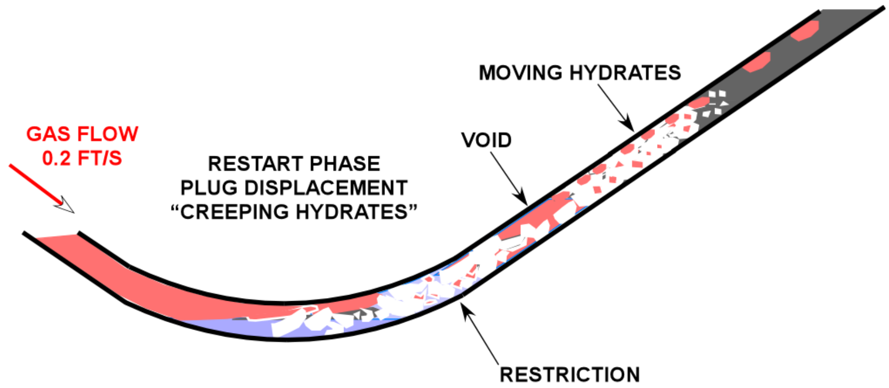

Figure 6.9f: As more of the pipe cross section is restricted with hydrates, the gas velocity increases as well as turbulence. Eventually, parts of the restrictions break off; the presence of hydrates along with the gas flow prevents the remaining liquid from draining back down.

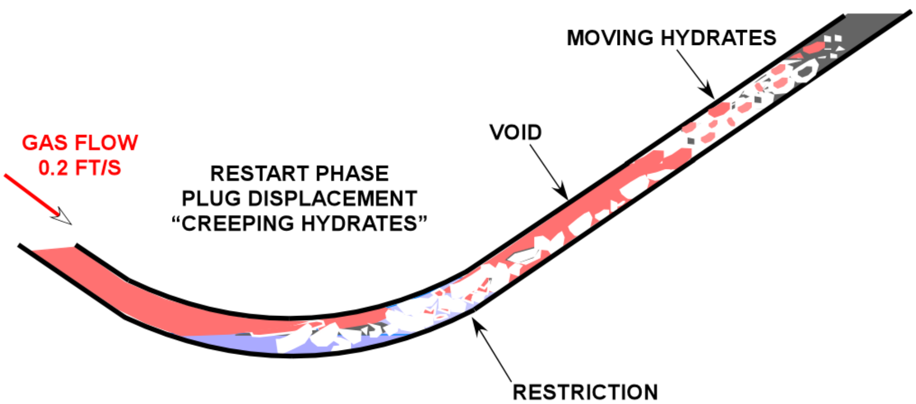

Figure 6.9g: After the restriction breaks off, the gas pressure acts as a piston on the restriction, pushing the hydrate and remaining liquid further up the pipe. Some hydrate agglomerates are left behind the "creeping" hydrate plug.

This mechanism has been inferred from visual observations as well as fixed and scanning gamma-densitometer data as shown on Figure 6.10.

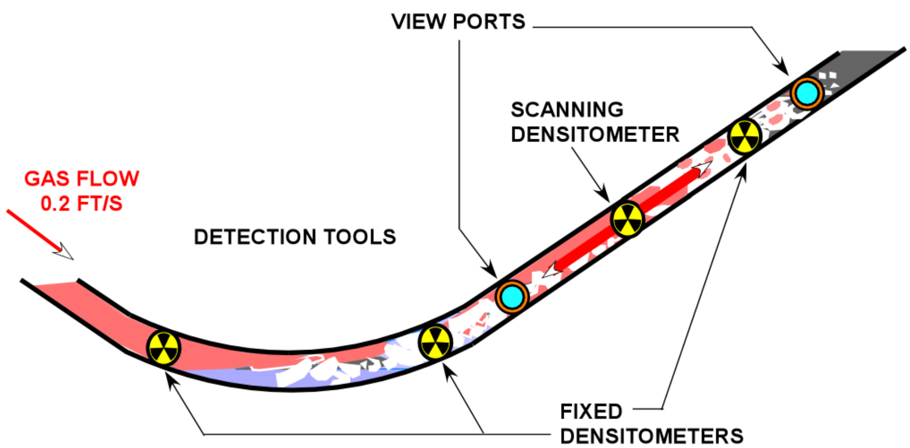

Figure 6.10: Location of detection instruments for low spot restarts

It should be noted that this mechanism has been observed with Citgo 19 and for water cuts of 50% only. Similar mechanism may take place with other fluids or conditions; however, this mechanism is most likely to occur for segregated cases and high water cuts. To illustrate the mechanism, Figure 6.11 shows pictures of hydrates in the top view-port of the uphill pipe section at time of 7, 8 and 11 minutes after restart.

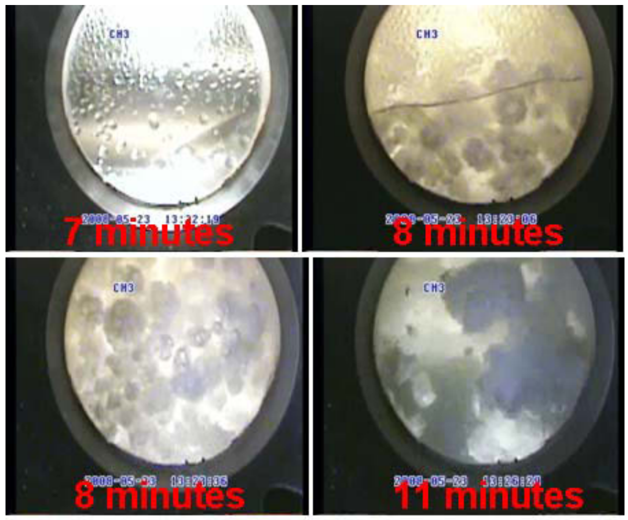

Figure 6.11: “Piston effect” due to hydrates upon restart

At 7 minutes, no hydrates are visible from the top view port. A minute later, the liquid interface appears at the view port. The liquid is being pushed up, with some slugging taking place, as a large hydrate restriction upstream in the section is being pushed up by the gas as illustrated above. Observations indicate that the liquid is loaded with hydrates; with time the size of these agglomerates increases as shown at 11 minutes.

Figures 6.12a to 6.12f show the scanning gamma-densitometer traces for the four salinity tests shown in Table 6.4 as a function of time. Figure 6.11a shows the expected density traces as a function of pipe content so the reader can better relate Figures 6.12b to 6.12g with what is happening inside the pipe during the restart.

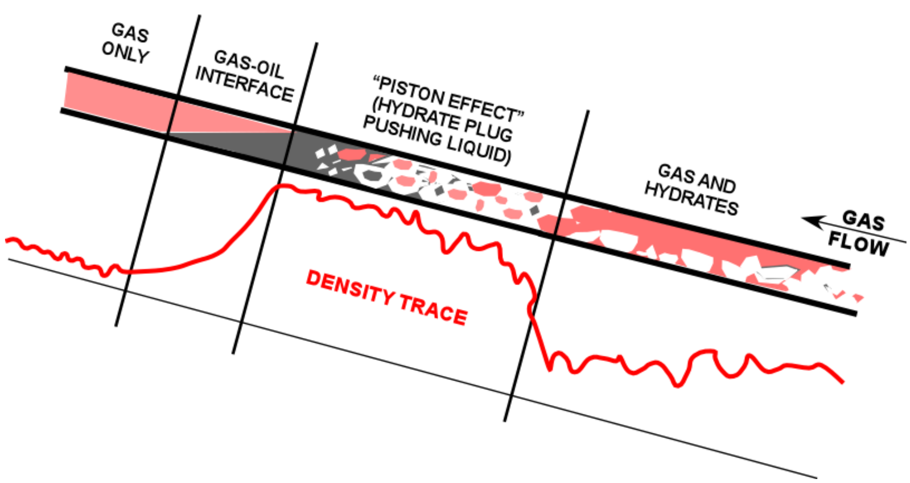

Figure 6.12a: Expected density trace based on pipe content

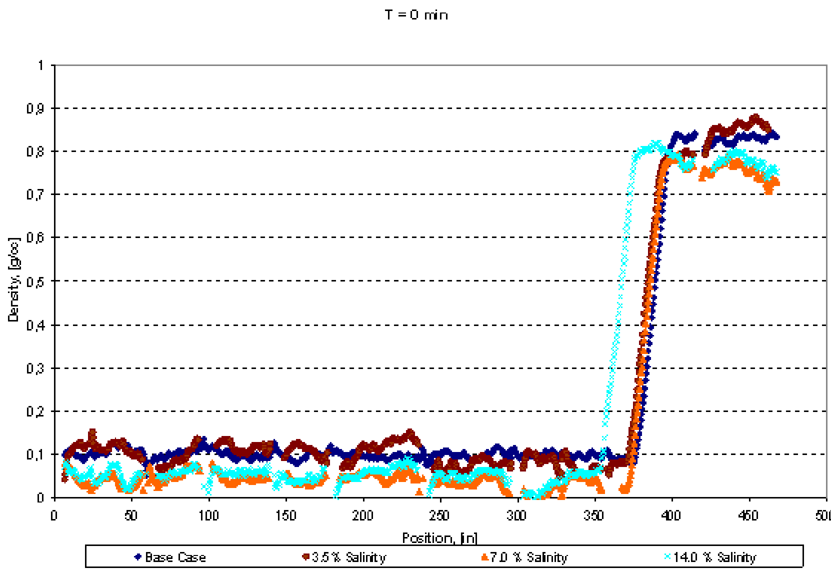

Figure 6.12b: Before restart, traces indicate the liquid level at the bottom of the pipe for different salinities tested.

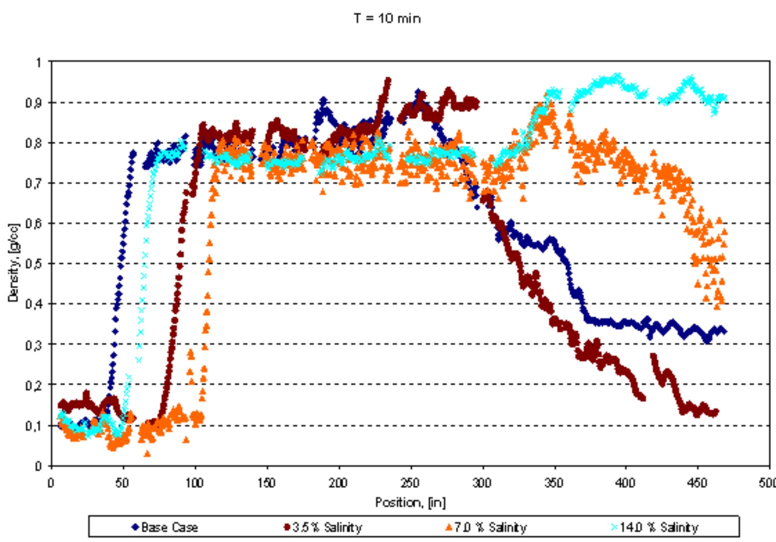

Figure 6.12c: At 10 minutes into restart, the liquid has been displaced by the gas. The liquid front is at the same level for all tests. However, lower salinity cases (fresh and 3.5%) already show a “piston effect” pushing the liquid up the leg, as may be shown by the decreasing density between 300 and 450 inches.

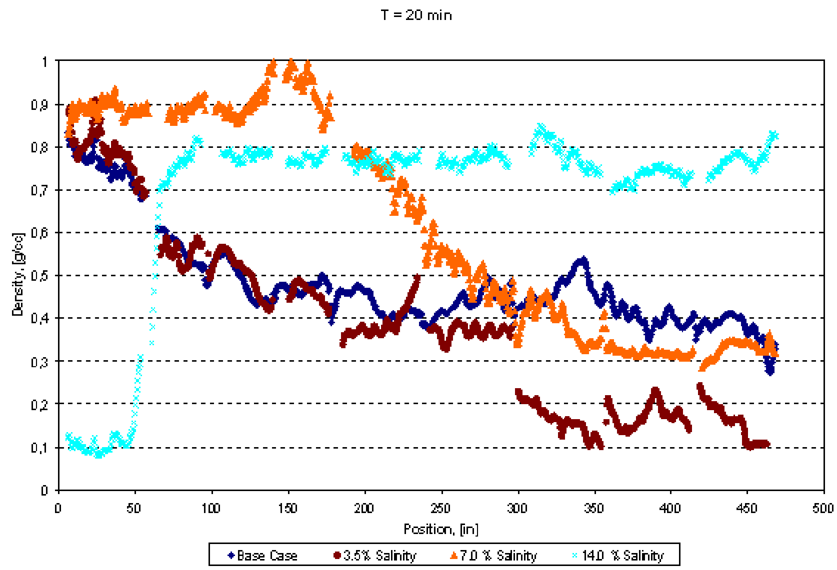

Figure 6.12d: At 20 minutes, the lower salinity cases (fresh water and 3.5%) have already displaced the liquid out of the scanning range. The 7% salinity shows the liquid displacement as started while for the 14% salinity case, no liquid or hydrate displacement is visible yet.

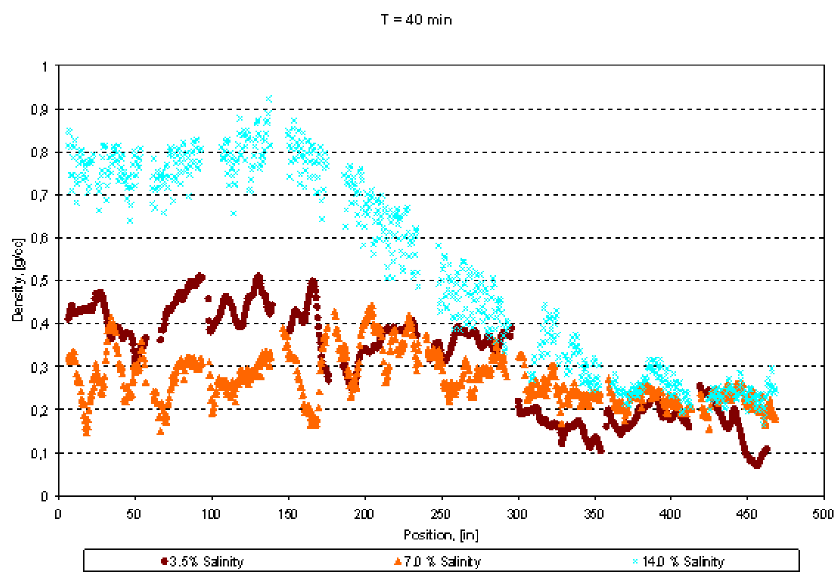

Figure 6.12e: At 40 minutes, the lower salinity cases have already displaced the entire remaining liquid out of the scanned region, while the 14% case is still in the process of "creeping" hydrates and remaining liquid.

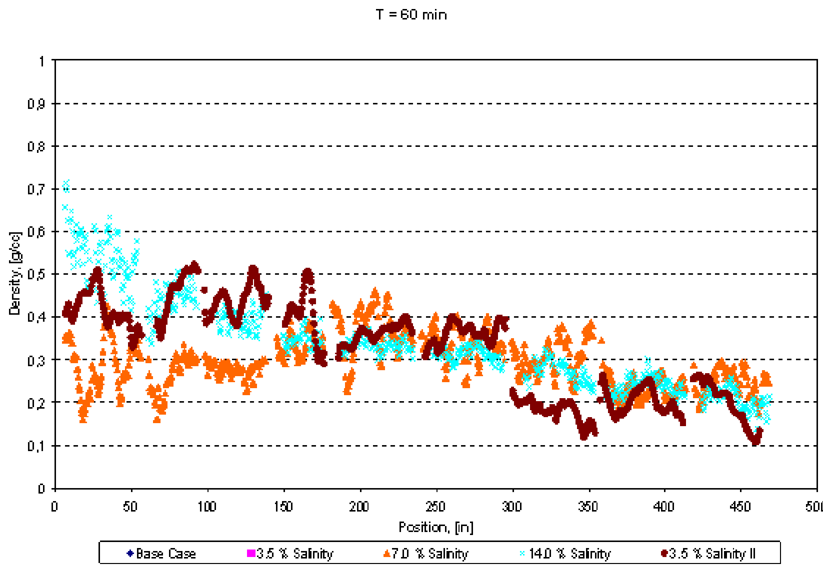

Figure 6.12f: At 60 minutes, even the higher salinity test has displaced the liquid/hydrates outside the scanning range.

Figures 6.12a through 6.12f illustrate the liquid/hydrate displacement observed and the mechanism explained on Figure 6.9a through 6.9g. The lower salinity cases resulted in a faster displacement of the hydrate/liquid mixture along the pipeline. Since during the restart experiments, gas is bubbling through the liquid column, the only way for the liquid to be pushed up the pipeline is through the formation of a hydrate restriction, acting as a piston to displace this liquid (mainly oil – the water being converted into hydrate). At higher salinity, it is known that hydrate formation rate is reduced because of the lower driving force (or lower sub-cooling) due to the presence of salt. This lower formation rate, combined with possibly other mechanisms due to the presence of salt, affects the morphology of the hydrate restriction, resulting in a slower formation or the formation of more permeable plugs for the higher salinity cases. Less permeable plugs would result in a more efficient piston effect displacing the liquid. Other effects, such as a different stickiness of hydrates for different salinities, could be at play in explaining the observed difference.

These experiments showed that the salinity had an effect on the formation rate of the hydrates, as well as an impact on the resulting flow patterns. Once again, these experiments showed that the understanding of transient flow patterns is one essential step for hydrate plugging studies under low-spot conditions.

6.3.3. Effect of liquid loading

All previous experiments were conducted with the flow loop charged with 25% liquid loading. This means that at 8 degrees inclined, the low spot is completely full of liquid. In addition, for water cuts of 25% or higher, and segregated conditions, the pipe cross section in the low spot is completely bridged with water. In other words, the in-situ liquid loading in the low spot (and sometimes the in-situ water fraction) is 100%. A couple of experiments were dedicated to investigate the effect of liquid loading, especially a non-bridged cross section, on the restart behavior. These experiments are shown in Table 6.5.

Test ID	Water cut (% Vol.)	Overall liquid loading (% Vol.)	In-situ liquid loading (% Vol.)	Angle (deg.)	Bridging conditions
NG-09	100	25	100	-8	Bridged
NG-10		4			
NG-11			85	-5	Non-bridged

Table 6.6: Non-bridging test matrix

The tests were conducted with water only and at the higher restart velocity of 0.25 ft/s to maximize the chance of displacing the water in the low spot. In order to keep the same amount of liquid in the loop for the bridged and non-bridged cases, the inclination angle of the loop had to be reduced to obtain non-bridged conditions. No differences were seen on pressure drops and the amount of liquid in the loop is too small to be captured by the scanning gamma-densitometer. Figures 6.13 and 6.14 show the fixed densitometer traces as a function of time for NG-10 (bridged case) and NG-11 (non-bridged case).

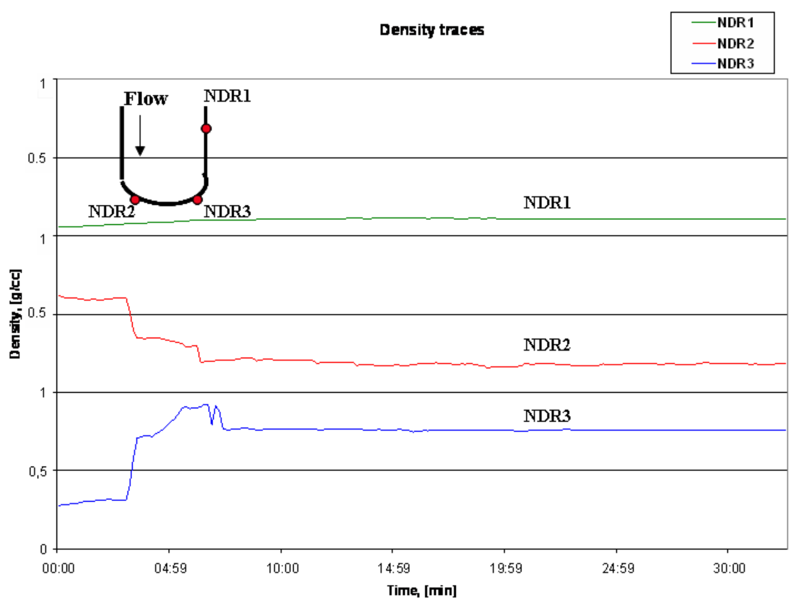

Figure 6.13: Density measurements for bridged case (100% in-situ liquid loading)

For the bridged case, density traces indicate that the water is being displaced in order to allow the gas to flow as shown by density traces NDR2 and NDR3 at the low spot. However, only a slight displacement of the water is observed for the non-bridged case; this small displacement was not sufficient to produce significant amounts of hydrates. Actually, after the gas flow was shut-off for this test, only a thin film of hydrates was observed at the gas-water interface, but no agglomerates could be seen or any restrictions detected.

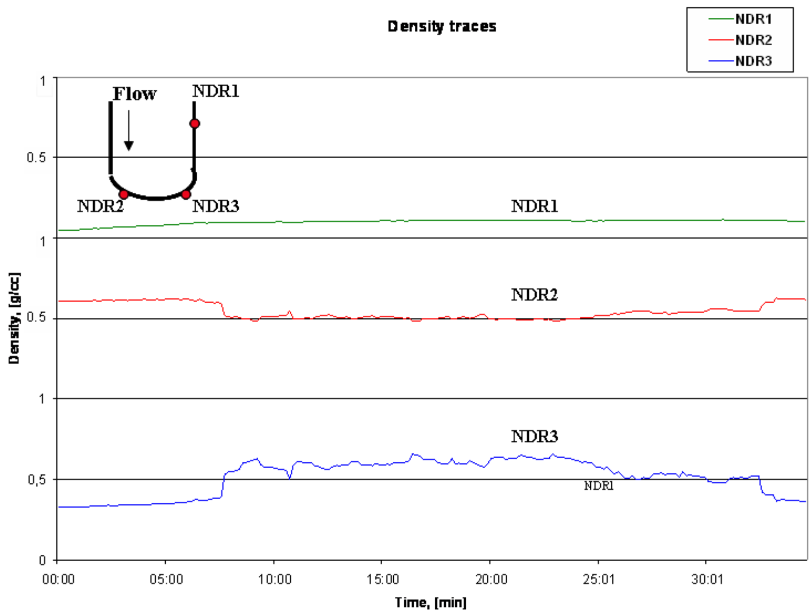

Figure 6.14: Density measurements for non-bridged case (85% in-situ liquid loading)

These non-bridging experiments show that the effect of liquid loading is tied to the gas velocity and to the geometry. If the gas rate and liquid loadings are not sufficient to displace the water, the risk of plugging is almost negligible. This is illustrated in Figure 6.15 below. However, if the gas rate or the liquid loading (or both) increase in such a way that a slug of water is displaced, the risk of bridging the pipe with hydrates – and therefore the risk of plugging – is increased, as shown in Figure 6.16.

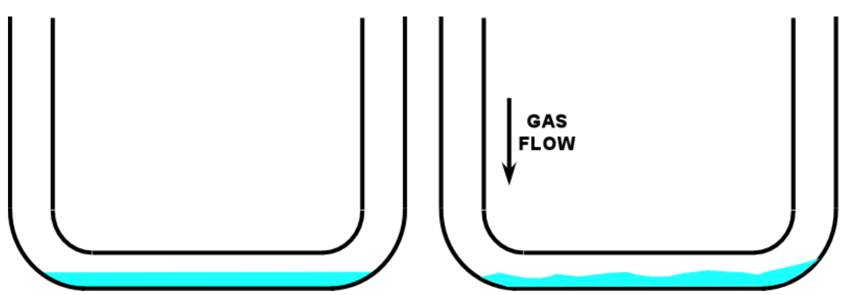

Figure 6.15: Non-bridged restart – Low liquid loading and low restart rate
(ripples on the liquid surface but no or little liquid carry-over – low risk of plugging)

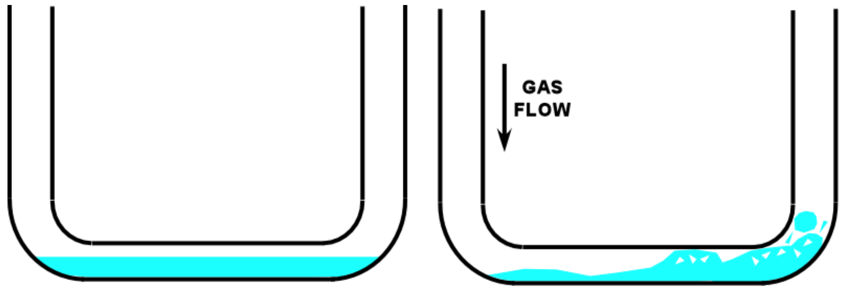

Figure 6.16: Non-bridged restart – High liquid loading or high restart rate (slugging and bridging occurs – higher risk of plugging)

These experiments were not conclusive, but illustrate once again the importance of the transient flow pattern, that is the combination of water cut, liquid loading, restart rate, phase distribution and system geometry. One can safely say that the risk of plugging a non-bridged pipe is much less than if the pipe is bridged; however, the authors believe it is possible to plug even a non-bridged pipe, depending on the operating variables and system geometry. More work is needed in this area.

6.4. Gas dominated restarts in low spots with anti-agglomerants

For planned shut-ins, rigorous operating procedures are implemented. For example, flow lines may be flushed with dead oil or inhibitors may be injected a few hours before shut-in. For un-planned shut-ins, however, procedure steps must be implemented – usually before cool-down to the hydrate formation region – to inhibit the flow lines or at the very least before the actual restart itself. One example would be the use of anti-agglomerants. Previous experiments at TUHFP have shown that – in all cases tested – implementation of anti-agglomerants with the recommended laboratory dosage was successful in preventing plugging. A few experiments were dedicated to verify that this statement applied to gas dominated restarts in low spots as well. These experiments were conducted with the Buttermilk fluid with a 35% water cut. The test matrix for these anti-agglomerant tests is shown in Table 6.6.

Test ID	Test conditions
BM-18	Blank test - No additive
BM-3A / BM-3AR	Base case - Oil and water mixed
BM-4A	Base case - Oil in water segregated
BM-5A	Base case - Slurry for BM-6A
BM-6A	Long term shut-in with hydrate slurry and additive
BM-7A	Injection of additive in upstream leg
BM-8A	Injection of additive in downstream leg

Table 6.7: Text matrix for anti-agglomerant tests

These tests were conducted with 35% water cut, a restart velocity of 0.15 ft/s and fresh water. The lab recommended dosage to prevent plugging under these conditions was 2.5% of the water volume. First, a blank test (BM-18) without additive was run, followed by two base cases (BM-3A and BM-4A) with the difference being in the charge procedure. Tests BM-5A and BM-6A were run to simulate a restart with additive followed by a 5-day shut-in; this simulates the case where a hydrate slurry is formed during the first restart and left to settle in the flow line for 5 days, with the intent of verifying that the anti-agglomerant would still be efficient after a 5-day shut-in. These tests also were aimed at verifying the possible aging of a hydrate slurry in the presence of anti-agglomerant. Finally, tests BM-7A and BM-8A tested a different anti-agglomerant charge procedure, with the additive injected pure into the downstream and upstream legs prior to cooling as shown in Figure 6.17. In these tests, the anti-agglomerant would have to drain and diffuse towards the water phase in order to be efficient during restart. In all other tests, the additive was mixed with the water charged into the flow loop.

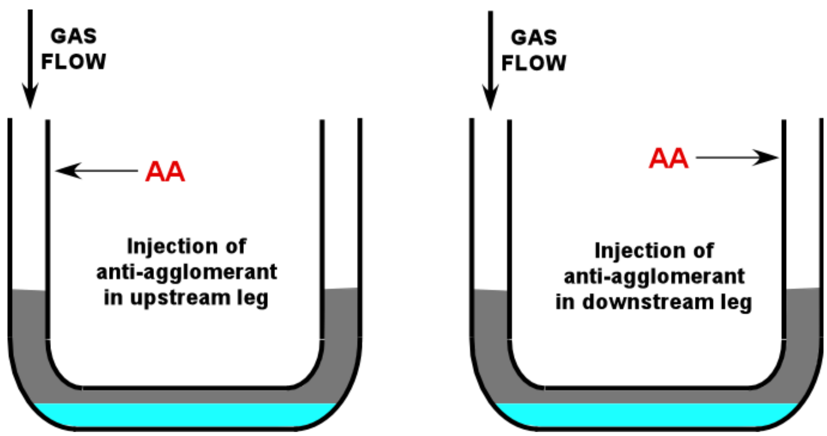

Figure 6.17: Different inhibitor injection strategies tested

Figure 6.18 shows the pressure drop traces for the non-inhibited case and the 3-hour and 5-day shut-ins. The uninhibited case shows that some agglomeration is taking place, resulting in a pressure drop increase in an irregular manner. Density scans indicated that restrictions were formed in the flow loop. Both additive tests showed an initial increase in pressure drop – corresponding to the fluids being displaced – followed by a constant pressure drop. Both additive tests were successful in keeping the hydrates dispersed. No difference was observed between segregated and dispersed conditions.

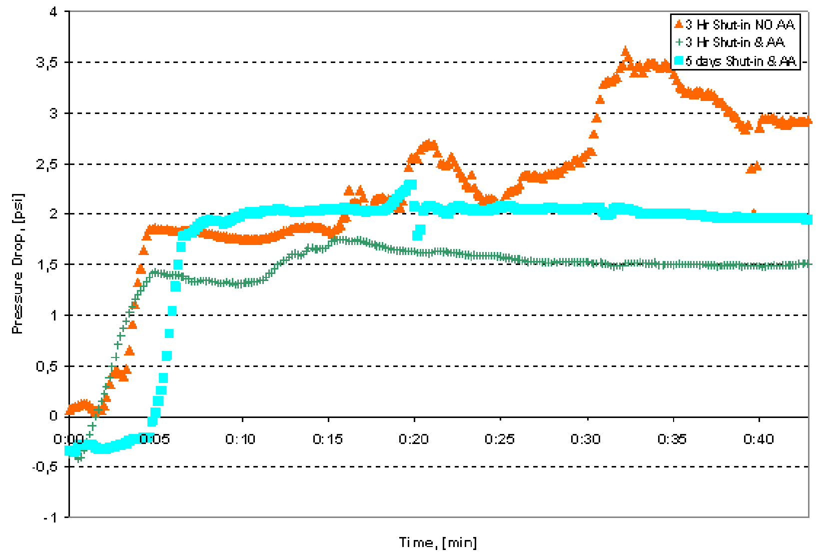

Figure 6.18: Pressure drop traces for inhibited and non-inhibited cases

Even after a hydrate slurry was formed and allowed to settle in the low spot for 5-days, the anti-agglomerant was effective in keeping the slurry dispersed during the restart phase. These experiments gave additional confidence that anti-agglomerants can be successfully deployed even for long shut-in cases, provided they are deployed with the right concentration and are perfectly dispersed in the water.

However, when the additive was injected after the shut-in, both tests (BM-7A and BM-8A) resulted in a fail. The additive could not reach the water phase and properly prevent agglomeration. This suggests that anti-agglomerants should be injected before shut-in and properly dispersed in the water phase to be effective. For both tests, the plug was located at the low spot.

7. Comparisons with OLGA5 simulations

To date, there are no models available to properly predict plug location and formation rate during restart conditions. To simulate hydrate formation in production systems, flow assurance engineers may use the CSMHYK-OLGA simulation code. CSMHYK is a hydrate kinetic module, capable of predicting hydrate formation rate, given the interfacial area and the sub-cooling. Coupled with the OLGA transient flow simulator, this module can predict hydrate formation in pipelines. However, the CSMHYK module is a steady-state simulator and validation data are required to evaluate the model performance under transient conditions. Finally, this state-of-the-art mechanistic model is applicable for dispersed systems only and does not represent segregated system very well. Here again, validation data is needed.

When this work was initiated, the CSMHYK-OLGA model was not commercially available so comparison with the model could not be made. Instead, in this work, comparisons were made with OLGA5 without the CSMHYK hydrate module. The objective of these simulations was to compare the location of plugs or restrictions to the predicted water volume fraction in the pipe.

The simulations were conducted with Citgo 19 model oil for the 25, 50 and 75% water cuts and both restart velocities. Results are presented in this section. Comparisons are made between scanning gamma-densitometer data (indicating the location of liquid/hydrate mixture) and water/liquid fractions in the pipe predicted by OLGA. The comparisons were made at two minutes into the restart phase as to get a close approximation before hydrates form (Figures 7.1 and 7.2) and at 30 minutes when significant agglomeration and restrictions have developed (Figures 7.3 and 7.4). Figures 7.1 and 7.3 compare the density measured by the scanning gamma-densitometer with the liquid density, weighed by the liquid holdup predicted by OLGA.

7.1 Simulations at 2 minutes

For the 25% water cut cases (both high and low velocity), the liquid displacement is fairly well predicted as shown in Figure 7.1. The noise-like fluctuations shown on the gamma-densitometer traces indicate that the loop is full of liquid with gas bubbling through the liquid column. Smaller fluctuations in the density traces indicate that larger amounts of solids are formed, as it is the case for the 75% water cut cases. At 25% water cut, the density predicted by OLGA shows that the water mainly remain below 80 ft. Observations indicated that restrictions were formed in the low spot sections, i.e. below 80 ft and out of the scanning range of the gamma-densitometer. For these cases, the plug location seems fairly well predicted when looking at the location of the water. A fair agreement is also shown for the 50% case at 0.25 ft/s velocity.

Larger discrepancies are observed for the 75% water cut case at 0.25 ft/s velocity and the 50% water cut case at 0.15 ft/s velocity. For the 50% case at 0.15 ft/s, the measured density trace indicate that a plug was formed between 80 and 95 ft, therefore pushing the remaining liquid from 95-ft to 115-ft. For the 75% case at 0.25 ft/s velocity, it seems that – as was observed during the salinity restart tests – a hydrate restriction was formed and displaced up the pipe, leaving behind material with a density of 0.4-0.5 g/cc. The simulations do not capture these effects since no hydrate module is coupled with this version of OLGA. For the 75% water cut and 0.15 ft/s velocity, the liquid density predicted matched the measured one, even though a plug was formed in this case.

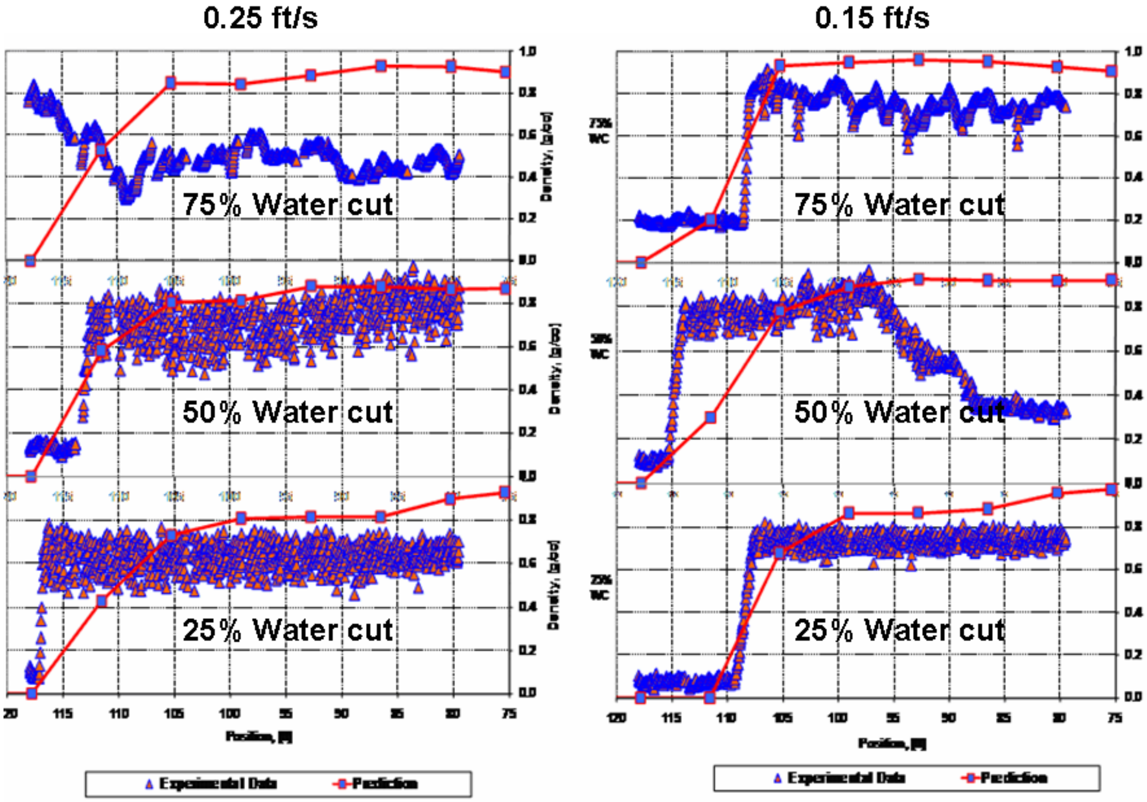

Figure 7.1: Experimental and predicted liquid front at 2 minutes into restart

These results indicate that OLGA predicts fairly well the initial liquid displacements. However, within a few minutes, as hydrates are formed, the predictions do not match the experimental data. Of course, the formation of hydrates increases the complexity of the restart flow patterns, which is not captured in this version of OLGA. Simulation models should account for hydrate formation as well as solid-liquid-liquid-gas flow patterns in a transient restart case.

Figure 7.2 shows the distribution of the liquids after two minutes into restart. The data is presented with decreasing velocity from left to right and decreasing water cuts from top to bottom. For the 25% water, most of the water is predicted to remain at the low spot, which agrees with the observations that the plugs were formed at the low spot section, outside the scanning densitometer range. For higher water cut, the liquid distribution is a mixture of water and oil, with significant water fraction along the pipe.

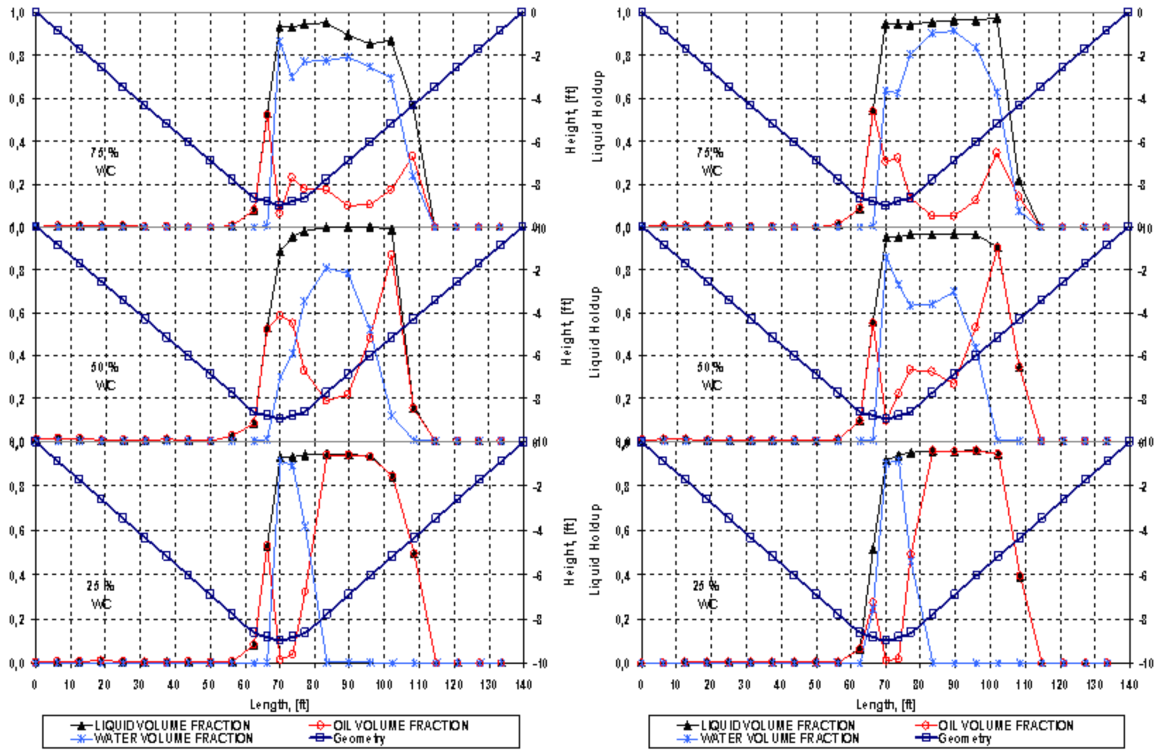

Figure 7.2: Simulated phase distributions at 2 minutes into restart

7.2 Simulations at 30 minutes

The OLGA5 prediction capabilities were additionally tested when comparing its prediction with actual data after 30 min into the restart. The results presented in Figure 7.3 identified the OLGA5 limitations in predicting liquid interfaces and densities with the presence of hydrates without a suitable hydrate module. It can be seen that the 25% water cut case at 0.15 ft/s was the only case properly predicted. As the water is converted to hydrates with time, more complex flow patterns are created and the solids may have a piston effect, pushing more liquid up the line. These effects are not properly predicted without a proper hydrate module.

After 30 min. into the restart phase, OLGA simulations indicate that most of the water settles back towards the low spot with oil accumulating on top as shown on Figure 7.4. This behavior might be representative in the case where no hydrates are formed. However, the presence of hydrates significantly modifies the flow patterns; the presence of solids accumulating may act as a piston, displacing the liquids further up the pipe where plugs form. Simulations with OLGA coupled with a hydrate module, might yield to better predictions; however, the complex 4-phase flow patterns may not be described properly by the existing models.

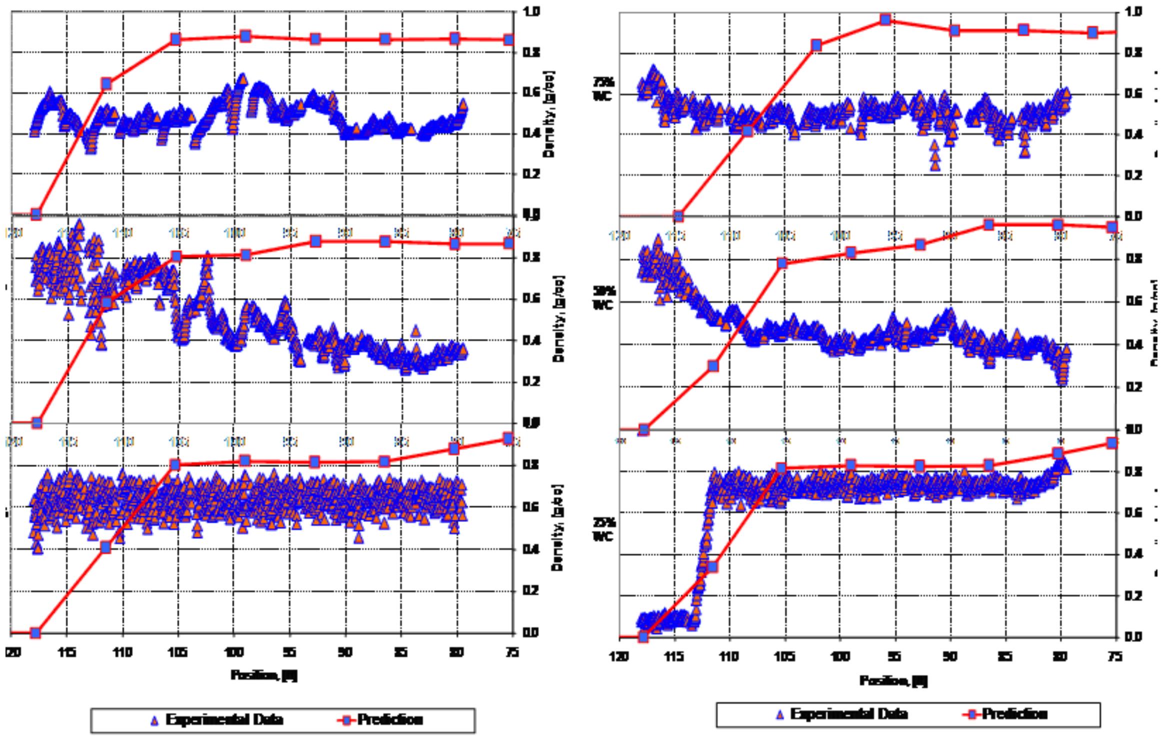

Figure 7.3: Experimental and predicted liquid front at 30 minutes into restart

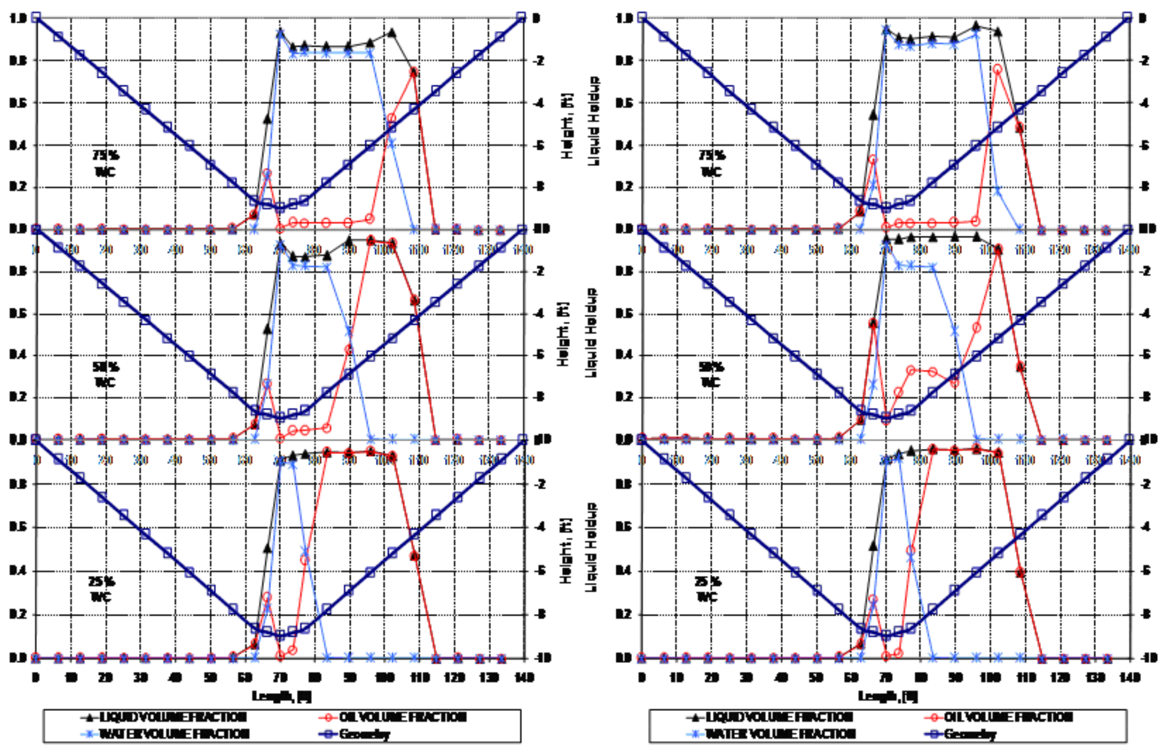

Figure 7.4: Simulated liquid distribution at 30 minutes into restart

These simulations indicate that the oil-water distribution may be predicted reasonably well by current state-of-the-art transient flow models. In other words, OLGA does a fairly good job in predicting water distribution, therefore showing where hydrate formation would be more critical. However, once hydrates start forming, the predictions do not match. Simulations with actual hydrate formation are required to properly conclude. Higher water cuts seem to increase discrepancies between simulations and experiments.

8. Plugging risk assessment

This study has highlighted some trends with respect to the hydrate plugging tendency of oil-water-gas systems upon restart. Table 8.1 shows how the risk of plugging changes with respect to some operating parameters. It is important to note that Table 8.1 describes the effect of each parameter individually and that combination of different parameters may have a different risk level.

	Plugging risk	
Parameter	**Lower**	**Higher**
Water cut	Low	High
Liquid loading	Low	High
Restart rate	High	Low
Diameter	Large	Small
Phase distribution	Dispersed	Segregated
Salinity	High	Low
Inhibitors	Yes	None

Table 8.1: Change in plugging risk with key parameters

Table 8.1 is a very simplified representation of the risk and combined effects of these parameters may yield different answers. For example, for high liquid loading, the risk may be evaluated as high; however, if the water cut is low (or extreme case zero), the risk may be low. Similarly, low water cuts and low liquid loadings may be evaluated as low risk; however, if the restart rate is high enough and the water phase is segregated, slugging may occur as shown in Figure 8.1. The slugging water may form hydrate and bridge the pipe somewhere downstream. The longer the horizontal section, the higher the risk would be since more water would be available to accumulate; geometrical considerations are equally important in evaluating the risk.

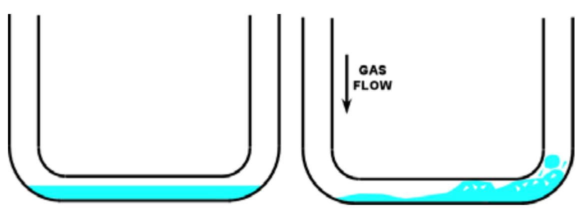

Figure 8.1: Slugging and plug formation at low water cut and low liquid loadings

As one can imagine, understanding and modeling of hydrate formation and plugging upon restart in low spots is very difficult and more data is needed to develop this understanding.

Work is on-going to develop a risk assessment methodology incorporating possible combinations of these variables as well as give values to the “high” and “low” conditions. The development of this methodology is only in its preliminary stages so it could not be reported at this time. Results will be made available to the MMS upon completion.

9. Conclusions

This study has highlighted some of the key factors involved in hydrate plug formation during restarts. These findings are summarized here.

- As expected, the risk of hydrate plugging increases with water cut.
- The risk of hydrate plugging is increased significantly if the water phase is segregated.
- Lower restart velocities promote plugging for both gas dominated and multiphase or liquid-dominated restarts.
- Higher velocities reduce the risk of plugging; the effect is increased if the water is dispersed in the oil phase.
- A mechanism of plug formation with gas restart and segregated water phase has been observed; hydrates and liquid were displaced towards higher sections of the pipe by a "piston effect" created by hydrate restrictions in the lower sections.
- As salinity is increased, the hydrate formation rate slowed down and/or more permeable restrictions were formed.
- Anti-agglomerants were successful in preventing plugging as long as the right concentration is used. They remained effective even after 5-days with a hydrate slurry present in the pipe.
- The injection strategy of anti-agglomerant is critical; even if injected at the right concentration, anti-agglomerants were not effective if injected after shut-in.
- Transient flow simulations perform reasonably well in predicting the liquid displacement and water distribution along the pipe. However, once hydrates form, simulations do not match. Also, the discrepancies are larger as water cut increases above 50%.
- These studies have emphasized that a deep understanding of the complex oil-water-gas-solid transient flow patterns taking place upon restart is required in order to understand and model hydrate formation and plugging accurately.

A preliminary risk analysis methodology is being developed from experience gathered during this study. A risk prediction tool is currently under development and will be made available to the MMS once completed. However, these experiments were limited by the current facility. Additional data and test conditions (especially higher gas restart rates, vertical sections…) are required to improve the technology in this area. A new riser facility is currently in its design phase at the University of Tulsa to expand the studies and the knowledge related to hydrate plugging during steady-state and restart operations.

Acknowledgments

The authors would like to thank the MMS and the members of the TU Hydrate Flow Performance JIP for the financial and technical support they provided for this work.